12-2014

Low Molecular Weight Glucosamine/L-lactide Copolymers as Potential Carriers for the Development of a Sustained Rifampicin Release System: *Mycobacterium smegmatis* as a Tuberculosis Model

Jorge Ragusa
University of Nebraska-Lincoln, jorgeragusa@gmail.com

Low Molecular Weight Glucosamine/L-lactide Copolymers as Potential Carriers for the Development of a Sustained Rifampicin Release System: *Mycobacterium Smegmatis* as a Tuberculosis Model

by

Jorge Alejandro Ragusa

A DISSERTATION

Presented to the Faculty of

The Graduate College at the University of Nebraska

In Partial Fulfillment of Requirements

For the Degree of Doctor of Philosophy

Major: Chemical and Biomolecular Engineering

Under the Supervision of Professor Gustavo Larsen

Lincoln, Nebraska

December, 2014

Low Molecular Weight Glucosamine/L-lactide Copolymers as Potential Carriers for the Development of a Sustained Rifampicin Release System: *Mycobacterium Smegmatis* as a Tuberculosis Model

Jorge Alejandro Ragusa, Ph.D

University of Nebraska, 2014

Advisor: Gustavo Larsen

Tuberculosis, a highly contagious disease, ranks as the second leading cause of death from an infectious disease, and remains a major global health problem. In 2013, 9 million new cases were diagnosed and 1.5 million people died worldwide from tuberculosis. This dissertation aims at developing a new, ultrafine particle-based efficient antibiotic delivery system for the treatment of tuberculosis. The carrier material to make the rifampicin (RIF)-loaded particles is a low molecular weight star-shaped polymer produced from glucosamine (molecular core building unit) and L-lactide (GluN-LLA). Stable particles with a very high 50% drug loading capacity were made via electrohydrodynamic atomization. Prolonged release (>14 days) of RIF from these particles is demonstrated. Drug release data fits the Korsmeyer-Peppas equation, which suggests the occurrence of a modified diffusion-controlled RIF release mechanism, and is also supported by differential scanning calorimetry and drug leaching tests. Cytotoxicity tests on *Mycobacterium smegmatis* showed that antibiotic-free GluN-LLA and polylactides (PLA) (reference material) particles did not show any significant anti-bacterial activity. The minimum inhibitory concentration and minimum bactericidal concentration values obtained for RIF-loaded particles showed 2- to 4-fold

improvements in the anti-bacterial activity relative to the free drug. Cytotoxicity tests on macrophages indicated an increment in cell death as particle dose increased, but was not significantly affected by material type or particle size. Confocal microscopy was used to track internalization and localization of particles in the macrophages. GluN-LLA particles led to higher uptakes than the PLA particles. In addition, after phagocytosis, the GluN-LLA particles stayed in the cytoplasm and the particles showed a favorable long term drug release effect in killing intracellular bacteria compared to free RIF. The studies presented and discussed in this dissertation suggest that these drug carrier materials are potentially very attractive candidates for the development of high-payload, sustained-release antibiotic/resorbable polymer particle systems for treating bacterial lung infections.

Acknowledgements

My most sincere appreciation and acknowledge to Dr. Gustavo Larsen, advisor and chairman of my committee, who guided and supported this adventure, and who provided a group atmosphere of critically, guided freedom in which to work. His extensive expertise of the various fields related to nanomaterials was an inspiration to me, and I was privileged to have been mentored by him. Thanks Gustavo for giving friendship, family and parenthood through this process.

An immense gratitude to the other members of my thesis committee: Dr. Pannier for many widely ranging suggestions and helpful comments; Dr. Subramanian for giving me the opportunity of working in her lab one summer, and publish our work; Dr. Velander for his friendly enthusiasm for my work and support.

I am deeply grateful to many associates and friends: Maciej Skotak, Sandra Noriega, Sumin Li and Daniela Gonzalez, for their collaborations, advise and support on this work. Thank you for your teachings and patience through this journey.

The support and love from my family and friends in Argentina have been a crucial factor for my mental health and interior peace. Thanks for always been aware. My love Daniela has been with me all these years and made them the best of my life. Besides being a splendid mom, she always had time to take care of me, and to be my partner, lover, best friend, mom and colleague. Thanks for being there those days when I needed you most.

Jorge

Table of contents

List of Figures viii

List of Tables x

CHAPTER 1 - INTRODUCTION

1.1. Synopsis 3

1.2. Motivation: Why Tuberculosis 5

1.2.1. Bacillus Mycobacterium Tuberculosis 6

1.2.2. Current Chemotherapy against Tuberculosis 7

1.2.3. Rifampicin (RIF) 8

1.2.4. Need for New Approaches to Combat the Disease 9

1.3. Background 10

1.3.1. Particulate Drug Delivery Systems 10

1.3.1.1. Drug release mechanisms and mathematical modeling 12

1.3.1.2. Drug Delivery Approaches for Tuberculosis Treatment 16

1.3.1.3. Electrohydrodynamics as a Tool for Fabricating Drug Delivery Carriers 21

1.3.1.4. Drug Delivery system: Cost analysis 26

1.3.2. Glucosamine L-lactide (GluN-LLA) 28

1.3.3. Antimicrobial Susceptibility Test 30

1.4. Approach: Ultrafine Particles as Drug Delivery System 31

CHAPTER 2 MATERIALS AND METHODS

2.1. Materials 35

2.1.1 Polymer Synthesis 35

2.2. Particle Preparation and Characterization 36

2.2.1 Particle Preparation 36

2.2.2 Size and Morphology 37
2.2.3. Drug Release Studies 38
2.2.4 Particle Degradation 38
2.2.5 Drug Encapsulation Efficiency 39
2.2.6. Thermal Properties of RIF Loaded Particles 40
2.3 Data Fitting and Statistical Analysis 40
2.4 Evaluation of Particle Effects on Bacteria 41
2.4.1 Bacterial Strain 41
2.4.2 Particle Toxicity on M. Smegmatis 41
2.4.3 Determination of Minimum Inhibitory Concentration (MIC) 42
2.5 Evaluation of Particle Loading Effects on Macrophages 43
2.5.1 Cell Line 43
2.5.2 Cytotoxicity of particles on macrophage cells 43
2.5.3 Particle Uptake, and Intracellular Localization by Confocal Microscopy 44
2.5.4 Intracellular Killing of M. Smegmatis 44

CHAPTER 3 – RESULTS AND DISCUSSIONS

3.1. Particle Fabrication: Optimization of Processing Conditions 48
3.2. Fabrication of Pure, and RIF-loaded Submicron- and Micron-sized Particles 52
3.3. Drug Entrapment Efficiency 59
3.5. Particle Degradation and Thermal Properties: Impact on Drug Release Kinetics 66
3.6. Particle Toxicity on M. Smegmatis 71
3.7. Minimum Inhibitory Concentration (MIC) and Minimum Bactericidal Concentration (MBC) of Free RIF and RIF Loaded Particles 74
3.9. Intracellular Localization of Particles by Confocal Microscopy 79

3.10. Intracellular Killing of M. Smegmatis 84

CHAPTER 4 – CONCLUSIONS AND FUTURE WORK

4.1. Conclusions 89

4.2 - Proposed Future Work 91

REFERENCES 102

List of Figures

Figure 1.1 - Rifampicin Chemical Structure 8

Figure 1.2 Glucosamine-L-lactide oligomer 30

Figure 1.3 - Basic electrospray apparatus 23

Figure 3.1. Control over particle size is achieved by varying the concentration of GluN-LLA 50

Figure 3.2. The effect of processing conditions, flow rate and voltage (A: 5 kV, B: 10 kV) on particle size and distribution 51

Figure 3.3. MP-GluN-LLA (A) and MP-LLA (B) were prepared at discrete voltages as indicated in respective plots. 55

Figure 3.4. SEM images illustrating the gradually changing morphology of polymeric submicronparticles made of low molecular weight polymers as RIF content is increased: 57

Figure 3.5. The effect of RIF loading expressed as polymer-to-RIF mass ratio, average diameter and particle size distribution. 58

Figure 3.6. Cumulative RIF release curves from submicron and microparticles. 63

Scheme 3.1. Representation of the bimodal kinetics of RIF release from the GluN-LLA carrier 65

Figure 3.7. Semi-log plot of degradation of submicron- (open symbols) and micron-sized particles (filled symbols) prepared using linear (left panel) and branched (right panel) L-lactide based polymers. 68

Figure 3.8. DSC thermograms. 69

Figure 3.9. Particle toxicity on *M. smegmatis*. 71

Figure 3.10. Particle cytotoxicity on Macrophages. 76

Figure 3.11. Internalization of particle by macrophages. 78

Figure 3.12. Intracellular localization of particles. 81

Figure 3.13. Intracellular killing of *M. smegmatis*. 85

Figure 4.1. First line anti-tuberculosis drugs 100

List of Tables

Table 1.1 – Rifampicin (RIF)-loaded particles made of synthetic polymers for pulmonary delivery treatment of tuberculosis. Particle diameter (Pd), drug loading (DL) 20

Table 1.2. Coefficient for equation 1.1 to determine droplet size 24

Table 3.2. Encapsulation efficiency and kinetic parameters of RIF release from L-lactide based polymeric submicron and microparticles (n = 3). 61

Table 3.3. MIC and MBC values of RIF in both free and encapsulated forms were determined by the macrobroth dilution technique. Particles were produced with a 1:1 RIF-to-polymer mass ratio. 74

Table 4.1 - Dual particle systems (PDS) proposed for future experimentation 91

Table 4.2 – Proposed Swiss mice groups for *in vivo* experimentation for oral and inhalation treatments. 94

CHAPTER 1

Introduction

CHAPTER 1

1.1. Synopsis 3

1.2. Motivation: Why Tuberculosis 5

1.2.1. Bacillus Mycobacterium Tuberculosis 6

1.2.2. Current Chemotherapy against Tuberculosis 7

1.2.3. Rifampicin (RIF) 8

1.2.4. Need for New Approaches to Combat the Disease 9

1.3. Background 10

1.3.1. Particulate Drug Delivery Systems 10

1.3.1.1. Drug release mechanisms and mathematical modeling 12

1.3.1.2. Drug Delivery Approaches for Tuberculosis Treatment 16

1.3.1.3. Electrohydrodynamics as a Tool for Fabricating Drug Delivery Carriers 21

1.3.1.4. Drug Delivery system: Cost analysis 26

1.3.2. Glucosamine L-lactide (GluN-LLA) 28

1.3.3. Antimicrobial Susceptibility Test 30

1.4. Approach: Ultrafine Particles as Drug Delivery System 31

1.1. Synopsis

This dissertation explores a new, custom-made polymer system as a promising drug delivery vehicle. Nano- and microparticles for tuberculosis treatment have been chosen as model system. This highly branched L-lactide grafted glucosamine (GluN-LLA) oligomer [1] was therefore processed into nano- and microparticles, resulting in nearly monodisperse particle size distributions. In addition, particles made from linear low- and high-molecular weight (LMW, and HMW, respectively) poly (L-lactic acid) (PLA) were produced and studied for comparison purposes. The most effective first-line anti-tuberculosis drug, rifampicin (RIF), was encapsulated in these nano- and microparticles via electrohydrodynamic atomization (EHDA). Particles were prepared from non-toxic or low-toxicity solvent solutions because fully biocompatible drug delivery systems are ultimately desired. Ethyl acetate, one of the better solvents in this class, has shown to be very effective for EHDA processing of L-lactide grafted chitosan [2]. For drug delivery applications, three of the most desirable traits of these GluN-LLA oligomers are their high solubility in EA, their tunable hydrophobicity-hydrophilicity balance via control of the length of the lactide substituents, and their LMWs

One of the most important problems with the current treatment of tuberculosis is the *low patient compliance* that causes multidrug-resistant (MDR) tuberculosis, and usually leads to patient death. A suitable solution to this problem is the implementation of a system that prolongs the therapeutic effect of one dose. In

order to demonstrate the sustained release of RIF from the new drug delivery system, *in vitro* release studies of RIF were conducted. Cytotoxicity effects of L-lactide, and GluN-LLA based particles were tested on macrophages. The bactericidal activity of encapsulated and free RIF toward the chosen model microorganism, *Mycobacterium smegmatis* (*M. smegmatis*), was evaluated. *M. smegmatis*, a non-pathogenic and fast growing specie (generation times of 3-4 hours), shares 2,000 homologs with *Mycobacterium tuberculosis (M. tuberculosis)*, which makes this microorganism the most accepted model to study *M. tuberculosis* [3]. The effects produced by the polymeric matrix were evidenced by the minimum inhibitory concentration (MIC) and minimum bactericidal concentration (MBC) values. Intracellular killing of *M. smegmatis* in macrophages, caused by RIF loaded particles, was also investigated. Confocal microscopy was used to determine the internalization and intracellular location of L-lactide and GluN-LLA based particles containing RIF into macrophages. Finally, the intracellular killing of *M. Smegmatis* in alveolar macrophages showed that the particles are able to maintain a sustained release of RIF into the cells with release rates affecting the bacteria death rate, further pointing to the potential of GluN-LLA as a possible new nanoparticle drug carrier for the treatment of tuberculosis.

1.2. Motivation: Why Tuberculosis

Tuberculosis, a highly contagious disease caused by the *M. tuberculosis*, ranks as the second leading cause of death from an infectious disease worldwide, after human immunodeficiency virus (HIV). According to the last report of the World health Organization (WHO) [4], tuberculosis approximately has infected 9 million people in 2013. In the same year, 1.5 million people died from this disease, including 360,000 HIV-positive patients. An estimated 1.1 million (13%) of the total new cases were HIV-positive.

Even though most cases of tuberculosis and death occur among men (60%) in their productive life stage, in 2013 there were an estimated 3.3 million new cases and 510000 deaths among women, and 550 000 infected with 80 000 death among children. These numbers reflect the high mortality of tuberculosis, which is unacceptably high given that most deaths are preventable. Tuberculosis can be cured in 90% of the cases that have access to the medication regimens of first-line drugs [4].

WHO Global Tuberculosis Report 2014 includes data compiled from 202 countries and territories. It shows that South-East Asia and Western Pacific Regions represents more than half (56%) of the estimated 9 million new cases in 2013. India and China alone accounted for 24% and, 11% of the total number of cases, respectively. The African region originated 25% of all cases, and also had the highest rates of fatal cases.

1.2.1. Bacillus Mycobacterium Tuberculosis

M. tuberculosis typically affects the lungs (pulmonary tuberculosis), but can affect other sites as well (extra-pulmonary disease), and is transmitted by aerosols from the lungs of coughing infected individuals. Exposure to these bacteria does not always translate into infection. It is estimated that bacteria is cleared by a robust innate immune response in 50% of the individuals exposed to *M.tuberculosis*. As for the rest of the infected population, only 5% progress toward the development of active tuberculosis, and the remaining 95% control the infection throughout their lives (latent tuberculosis) [5]. About one-third of the world's population (approximately 2 billion people) has latent tuberculosis, which progresses to the active disease when a patient's immune system is compromised by say, HIV infection, old age, immunosuppressive drug treatment, or re-infection [4–7].

M. tuberculosis is a relatively slow-growing microorganism with a generation time of 24 hours. Infection is spread via airborne dissemination of aerosolized bacteria containing droplet nuclei of 1-5 μm [7]. *M. tuberculosis* bacteria that gain access to a new host via inhaled air can begin the replication process inside the alveolar macrophages after 2-3 weeks of infection. Macrophages usually ingest and trap pathogens in a phagosome, which is then subject to a series of fusion and fission events with the endocytic pathways that end in a phagosome-lysosome fusion. This process is known as phagosome maturation, in which phagosomes acquire the antimicrobial tools to eliminate the pathogen. These killing mechanisms include acidification (pH<5), production of antimicrobial peptides, generation of

reactive oxygen and nitrogen species, and degradative enzymes such as cathepsins. However, *M. tuberculosis* is able to modulate pH-reducing events in a maturing phagosome, which can result in a more basic phagolysomal pH, thus enhancing bacteria survival and facilitating dormancy. The general view is that *M. tuberculosis* arrests phagosomal maturation by inhibition of both lysosomal fusion and reduction of recruitment of vacuolar H+-ATPases. These manipulations over the normal course of phagosomal maturation result in a modest drop of intrasomal pH, which avoid bacteria killing and favors its replication [5,8].

1.2.2. Current Chemotherapy against Tuberculosis

Mortality rates of tuberculosis fall between 50 to 80% in untreated patients and drop to 5% for individuals receiving an active therapy [4,7]. The current treatment, tuberculosis chemotherapy, requires six months of an extensive drug regimen of RIF, isoniazid (INH), pyrazinamide (PYZ), and ethambutol [7]. The treatment comprises the following two stages: (1) an intensive 2-month daily use of the four drugs mentioned before followed by (2) a 4-month daily administration of RIF and INH. This long and intensive treatment is one of the main causes for low patient compliance, and failure to adhere to the prescribed drug regime has resulted in the significant emergence of drug resistant strains of *M. tuberculosis*. Multidrug-resistant (MDR) tuberculosis has become a complex problem due to the recent proliferation of such strains. Treatment of MDR tuberculosis takes longer than conventional treatment modalities (WHO recommends 20 months), and requires more expensive and toxic drugs with lower success rates [4,9,10].

1.2.3. Rifampicin (RIF)

Rifampicin (Figure 1.1, formula: $C_{43}H_{58}N_4O_{12}$) is a semisynthetic derivative of the rifamycins, which are a class of antibiotics derived from fermentation products of *Nocardia mediterranei*. RIF possesses a unique mechanism of action that confers it a high level of antibacterial activity and it is based on the inhibition of bacterial RNA polymerase. By this action, RIF stops bacterial growth in a wide range of bacteria, including mycobacterium tuberculosis [11].

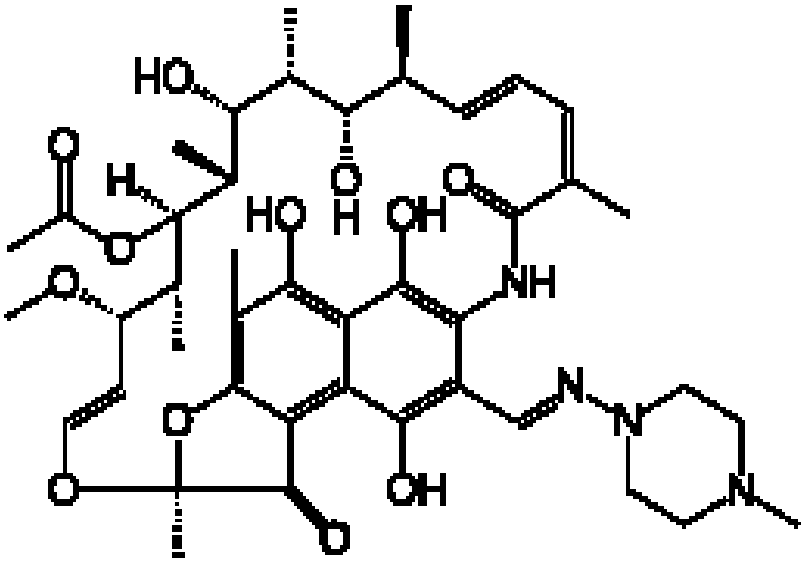

Figure 1.1 – Rifampicin Chemical Structure

1.2.4. Need for New Approaches to Combat the Disease

Usually, patients fail to take the prescribed medications with adequate regularity and duration. In spite of the fact that current anti-tuberculosis chemotherapy treatment is highly effective in killing *M tuberculosis,* it involves a multidrug regimen where patients have to take a significant number of pills daily (up to eight at one time) for a long time. This is the main reason for patient non-compliance, but the appearance of side effects is also cited. With the current treatments, only a small fraction of the dosed antibiotics reach the target area, mainly because its first-pass metabolism decreases the amount of drug that gets into the blood stream. As a consequence, to achieve therapeutic levels large doses of drugs are normally needed, and the probability of patients experiencing side effects increases [12]. Hepatotoxicity, the most common side effects of anti-tuberculosis drugs, generally leads to treatment withdrawal [7,13]. These difficulties associated with patient non-compliance are the main driver behind new research aimed at exploring new drug administration concepts. Multiple new drugs and vaccines are in the pipeline or are being investigated nowadays, but neither route guarantees success [14], nor do they go against conventional treatment paradigms.

An alternative strategy to current treatment approaches is to encapsulate anti-tuberculosis drugs in nano- or microparticles made from biodegradable polymers. For instance, a very effective treatment should target alveolar macrophages where *M. tuberculosis* is harboring via suppression of the phagosome-lysosome

fusion process [15]. Since alveolar macrophages are one of the first lines of defense against entry of external particles including microbial invasion, macrophages targeting is generally accomplished even without any specific tailoring of the particles [16]. Therefore, in this work, drug delivery systems comprising RIF-loaded nano- and microparticles made from two biodegradable polymers (GluN-LLA and PLA) are presented as a potentially new strategy to treat tuberculosis.

1.3. Background

This section presents basic background material which will be relevant to more specific discussions in subsequent chapters.

1.3.1. Particulate Drug Delivery Systems

Generally, conventional drugs are low molecular weight substances capable of crossing body barriers and accessing numerous cell types and subcellular organelles. Although this aspect represents a desired feature for the treatment of diseases, it also implies an indiscriminate distribution of the drug to an uncontrollable extent of the body. As a consequence of this drug ‘dilution’ in the body, higher doses of the therapeutic agent are required for a satisfactory pharmacological response, which usually carry undesired side effects on the patient. Rapid renal clearance of drugs requires frequent administration, threatening, especially in long-term treatments, the compliance of the patients [17]. Compliance is crucial for curing tuberculosis. Standard multi-antibiotic

treatment results in systemic delivery of the drugs throughout the body; drugs are rapidly detoxified and/or excreted, and daily doses are required. RIF, INH and PYZ, first-line anti-tuberculosis drugs, are metabolized by the liver and induce hepatotoxicity. This adverse effect is of primary concern, because it often requires changes in the treatment [13,16].

Controlled-release drug delivery systems are designed to provide adequate doses of therapeutic agents for a relatively long period of time, to the proper location, in an effective manner to increase compliance and minimize side effects [18]. These systems employ devices that are capable of releasing drugs by reproducible and predictable kinetics. Biodegradable polymeric nano- and microparticles are among the most investigated types of devices as drug delivery vehicles. Some of their advantages are, (1) drug release rates can be tailored to the need of a specific application, (2) protection of the drug from degradation and clearance, especially proteins, with lower required doses, (3) improved patient comfort and compliance by decreasing the frequency of doses, for example, sometimes even from daily to weekly doses, and (4) localized, targeted delivery of the drug to minimize side effects [17–19]. Controlled-release particle formulations that maintain a constant level (zero-order release kinetics) of a drug for long periods of time i.e, effectively prolonging the therapeutic effect of one dose, is the ultimate long-term goal in developing the drug carrier systems presented in this dissertation. These formulations are often referred to as “sustained release”, or “prolonged release formulations” [20]. One critical concern with orally administering RIF is its bioavailability in the acidic environment of the

stomach. RIF displays decomposition rates between 8.5 to 50% in the corresponding gastric time for most treatment modalities in humans (~15 to 105 ± 45 min) [21,22]. The entrapment of RIF inside ultrafine particles serves not only as a means to develop a slow-release reservoir system, but also as protection from degradation, which in principle solves the RIF bioavailability issue [7].

1.3.1.1. Drug release mechanisms and mathematical modeling

Several factors affect release rates in nano- and microparticles, such as mode of drug entrapment, polymer type and its molecular weight, copolymer compositions, polymer matrix-drug interactions, excipients, particle geometry, and physicochemical and biological properties of the active and carrier ingredients, among others [17,18,23,24]. Drugs can be encapsulated inside a "core" or reservoir surrounded by a thin polymer "shell", or can be uniformly dispersed or dissolved in the polymer matrix. These two different drug entrapment modalities are usually defined by the type of particle being designed for, i.e., core-shell or solid particle. The polymer type and its molecular weight are governing elements affecting the mechanism by which the drug is released from the particles. These factors strongly influence particle characteristics like degradation rate, swellability and polymer matrix interaction with the drug [24]. In this dissertation, RIF was dissolved in GluN-LLA and PLA matrix, and four particulate drug delivery systems were produced. Drug release studies and mathematical modeling from this data are used to assess the relative importance of drug-matrix interactions.

Numerous mathematical models that predict polymer drug delivery behavior have been reported over the last few decades [25]. The classic Ritger and Peppas equation $M_t/M_\infty = kt^n$ [26] is a simple exponential form that can be used to fit drug release kinetic data. In the equation, M_t/M_∞ is the drug cumulative release percentage at time (t), *k* is the rate constant, and *n* is the so-called diffusional exponent. Both *n* and *k* are determined by the principles governing diffusion, degradation, relaxation, matrix-drug interaction, and geometry of the drug delivery system. Fickian-type diffusion of a drug for example, is driven by a chemical potential gradient. Relaxational release refers to systems possessing a swellable matrix, and is mostly hydrophilic polymers. In this particular case, the carrier's polymer chains "relax" upon contact with water or biological fluids, and this facilitates drug delivery by increasing its mobility across the matrix.

In the pharmaceutical field, data from drug release experiments are generally fitted to the Ritger and Peppas equation, and the obtained *n* value is used to propose a drug release mechanism [25]. For spherical particles, a pure Fickian diffusion controlled-release system is described by n=0.43, while n=0.85 is related to swelling-controlled drug delivery mechanism. Values of *n* between these two numbers represent drug release systems controlled by both diffusional mass transport, and chain relaxation. The case of n=0 correspond to a zero-order drug release process, and is related to systems displaying pure biodegradation-controlled behavior, where drugs are strongly entrapped (e.g. covalently bonded) within the polymer matrix [27]. Values of *n* between 0 and 0.43 represent an overlap of drug-matrix interaction and diffusion mass transport mechanisms [27].

Since Ritger and Peppas equation does not fit data well in cases where high degradation rates occur, other mathematical models may be adopted. Biodegradable polymers are widely used in the design of nano- and microparticles as controlled drug delivery systems. Polymer degradation routes can be divided into two different categories: bulk-eroding and surface-eroding degradable systems. Numerous mathematical models that apply to degradable systems can be found in the literature [19,28].

For the sake of illustration, one can picture a model solid nanoparticle having the drug uniformly dispersed in a degradable copolymer matrix, and the different possible mechanisms of controlled drug delivery systems. Case 1: the rate of degradation is *slow enough* for the particle to be taken as non-degradable during the release period, and the matrix does not either swell or presents no important interaction with the drug. This drug delivery system would probably be controlled by pure Fickian diffusion (n=0.43) [26]. Case 2: swellability effects in the polymer matrix are large enough that when water diffuses into the particle, polymer chains relax and drug is released by a swelling-controlled process (n=0.85) [29]. Case 3: very strong drug-matrix interactions or polymer-drug conjugates are formed. Drug release depends only on biodegradation or chemical erosion to free the drug from the particle (n=0). These three situations represent the three extreme cases of drug delivery i.e., a process governed by one single phenomenon (diffusion, relaxation and degradation). Systems that are controlled by a combination of two or more phenomena are all too common, e.g. diffusion and relaxation coupling ($0.43<n<0.85$) [30]. Values of n between zero and 0.43 are generally taken as

indicative of diffusion and matrix-drug interaction mechanisms being present. Matrix-drug interactions are most likely responsible for strong delaying effects in observed drug release profiles. In this last case, the polymer matrix does not undergo swelling, and the carrier's degradation rate is also not an important factor.

In this dissertation, GluN-LLA nano- and microparticles particles have been produced, with the goal of functioning as controlled-release drug delivery systems. Since their biodegradation rates were relatively modest (see Chapter 3), it was not considered to be an important factor in the modeling of the release process. Due to GluN-LLA particles containing a larger proportion of L-lactide molecular building blocks relative to their glucosamine core unit, this copolymer was a priori viewed as a good non-swelling system. Therefore, the Ritger and Peppas equation was viewed as a viable candidate to model the drug release profiles.

Frequently, especially for prolonged release products, there are three basic stages in a time-release profile: (1) initial burst of drug release, taking place during the first few hours, followed by a (2) slow diffusion-controlled release, and finally, a (3) phase where drug is released faster as a consequence of degradation start playing a pivotal role. Burst release is usually linked to drug diffusion from the outermost layers of the particles. In some cases, degradation can be controlled to a good extent by varying the ratio of the monomeric building blocks in copolymers. For example, poly(lactic-co-glycolic) (PLGA) degradation

rates can be increased by having higher glycolic acid contents [20]. Despite the observed differences between drug release phases one and two (chapter 3), RIF release profiles from GluN-LLA and PLA particulate systems showed no phase three during the observation period (~14 days). This also suggests a slow degradation rate.

1.3.1.2. Drug Delivery Approaches for Tuberculosis Treatment

As mentioned in Section 1.2, tuberculosis chemotherapy requires the administration of a multi-drug regimen over a long period of time. Low patient compliance is the main reason for treatment failure, which in turn frequently causes MDR tuberculosis and/or patient death. In order to improve compliance, minimize toxicity and to increment RIF bioavailability in tuberculosis treatment, efforts have been made to develop drug delivery systems composed of nano- and microparticles.

Various drug carriers derived or purified from natural sources such as chitosan [31], alginate [32,33], gelatin [34], fatty acids (Pheroid technology) [35] and synthetic encapsulants, such as poly(lactide-co-glycolide) (PLGA) and poly-D,L-lactide (PDLLA) have been used in anti-tuberculosis drug encapsulation. RIF is one of the first-line antibiotics being used in treatments of tuberculosis, and is usually employed when investigating new particulate systems. A review of the recent literature on RIF controlled release systems reveals that the most popular drug carriers still belong to PLGA family [12,36–47]. For studying a subcutaneous

injection approach, Dutt et al. [44] produced PLGA microparticles containing RIF and INH by the double emulsion evaporation technique and particles size was 11.75 μm and 11.64 μm respectively. The particles were administered in a single dose subcutaneously to mice; the microparticles sustained a therapeutic release of the drugs for 7 and 6 weeks for INH and RIF respectively. As an observation, authors showed that particles with diameter > 10 μm remained at the site of injection, forming a depot where drugs were released via diffusion processes. Such a depot can release drugs over several weeks, while the same dose of free drugs were present *in vivo* only for 24 hours. It needs to be indicated however, that subcutaneous and intravenous routes of administration involve injections, which in turn lead to additional patient pain and discomfort. This tends to favor the development of oral and inhalation drug delivery systems as being more convenient to patients and as a natural result, more research has been reported for the oral and inhalation drug administration routes.

As an oral formulation strategy, *Ain et al.* [45] used a double emulsion technique to encapsulate RIF, INH and PYZ in PLGA microparticles with a size range distribution between 1.1-2.2 μm. These particles were administrated orally in mice, and drug concentrations achieved via use of microparticles were compared with those resulting from use of the free drug. In all cases, encapsulated drugs remained present in circulation for up to 72 hrs after dosage, while administration of free drugs led to their elimination within 24 hrs. *Pandey et al.* [47] prepared RIF, INH, PYZ loaded PLGA nanoparticles by the multiple emulsion technique obtaining a particle size range between 186-290 nm, with a drug encapsulation

efficiency of 56.9±2.7 %. Drug levels in plasma reached therapeutic values for 6-8 days and for up to 11 days in the lungs with a single dose administration to guinea pigs. Even though use of drug-loaded microparticles leads to lower doses and lower administration frequency via the oral route than when the free drugs are administered, first-pass metabolism is still a concern. This phenomenon (also known as first-pass elimination or presystemic metabolism) refers to the drug fraction that is metabolized after its administration, and before it is effectively utilized at the desired therapeutic site. The primary organ involved in first-pass metabolism of an orally administered drug is the liver, other areas with less impact on first-pass metabolism are the gastrointestinal tract, blood, vascular endothelium and lungs [48].

In the case of pulmonary drug delivery, inhalation therapy has the added advantage of being capable of releasing the anti-tuberculosis drugs right at the main site of infection, where alveolar macrophages harbor *M. tuberculosis* bacteria inside the phagosomes. In addition, inhalation therapy has the inherent benefit of chiefly bypassing first-pass metabolism, thereby allowing elevated local concentrations of the drug where it is most needed, and without requiring high drug concentrations in circulation. This, in turn, reduces systemic toxicity risks. Via the inhalation route, it is also possible to achieve systemic therapeutic concentration of the drugs [7,49]. This is important in that tuberculosis is a systemic disease that primary affects the lugs, but can also affect other areas as well such as the liver, kidney and spleens. There are a considerable number of publications in the open literature that propose formulation of anti-tubercular

drugs into nano- and microparticles for pulmonary delivery. In spite of the fact that first-line drugs are the ones that are predominantly used, other second- and third-line anti-tubercular drugs have been investigated [7,49,50]. RIF alone has been encapsulated in PLGA microparticles mostly by means of two techniques: double emulsion [46,51,52] and spray drying [12,52,53]. RIF has been also encapsulated in combination with other first-line anti-tuberculosis antibiotics, especially with INH and PYZ [47,51,54]. Table 1 shows what are believed to be the most relevant published research in RIF-loaded microparticles made out of synthetic polymers for pulmonary delivery treatment of tuberculosis. As it can be observed, values for drug loading (DL) capacity vary between 10-30% for PLGA and 8-16% and for PLA microparticles. Other natural materials such as chitosan [31], alginate [32], and gelatin [34] were also employed to encapsulate RIF, and showed DL of 8.9-46.3%, 25-37%, and 42%, respectively. In this dissertation, stable RIF-loaded particles presenting DL of 50% were produced by the electrospray technique. This superior characteristic of GluN-LLA systems is attributed to the fabrication method (next section), and the physicochemical properties of the polymer that promote high drug-polymer interactions (Chapter 3).

Table 1.1 – Rifampicin -loaded particles made of synthetic polymers for pulmonary delivery treatment of tuberculosis. Particle diameter (Pd), drug loading (DL)

Ref.	Manufacturing method	Pd (μm)	Carrier	DL (%)	Drug release and comments
[52]	Emulsion	3.45-6.84	PLGA	20	*In vitro* release 34% in 24hrs
	Spray drying	2.76	PLGA	30	*In vitro* release 74% in 24hrs
[12]	Spray drying	2.87	PLGA	30	*In vitro* release 52% in 24hrs
[42]	Spray drying	1.5 and 3.5	PLGA	10	Phagocytosis dependency on particle size: 80% uptake 3.5 μm microparticles.
[41]	Emulsion	2.84	PLGA	10	Drug release accelerated by pulmonary surfactant (release 50-90% in 24 hrs)
[55]	Supercritical anti-solvent process	3.29	PLA	8-16	Optimization of fabrication method conditions. Release 30-100 % in 24 hrs)
[53]	Spray drying	2.76	PLGA	-	Intracellular RIF from particles containing 0.25 and 2.5 μg RIF/mL were 2 and 10 times higher than 5 μg/mL of free RIF – ~50 % intracellular killing after 7 days

1.3.1.3. Electrohydrodynamics as a Tool for Fabricating Drug Delivery Carriers

Over the past few decades, there has been a growing interest in developing biodegradable nano- and microparticles as drug delivery systems. There are several methods for making ultrafine particles, such as emulsification-evaporation, salting-out/emulsification, nanoprecipitation, ionic gelation, coacervation, spray-drying and electrospray, among others [56–58]. As it can be deduced from Table 1.1, for pulmonary delivery of RIF, the emulsion/solvent evaporation and spray-drying methods are the ones that are most frequently used.

Solvent evaporation and emulsion-based methods are commonly used to prepare ultrafine particles, especially at lab scale. The emulsification/solvent evaporation technique involves emulsification of a dispersed phase in which the polymeric matrix and the drug have been dissolved or dispersed. The two phases are emulsified at high sheer rates, until the solvent evaporates and particles are formed [50]. RIF-loaded PLGA microparticles of diameters in the 3.5 to 6.5 μm range for pulmonary delivery were prepared using this method by O'Hara and Hickey [52]. Methylene chloride and polyvinyl alcohol (PVA) were used as dispersant and emulsifier, respectively. The two phases were mixed at 5000 rpm for 45 min, and particles were collected by filtration. However, emulsion-based methods possess a number of important disadvantages have limited their application. Large-scale production poses great technological difficulties, and is cost-prohibitive. Particle size distributions are usually broad, and standard

deviations of 50% are not uncommon. This, in turn, makes consistent drug release profiles difficult to obtain. Drug exposure to organic solvents, high temperatures and high shear stresses could potentially decrease, or in some cases eliminate drug viability, especially with delicate biomacromolecules. In addition, toxic compounds such as some of the additives and/or surfactants used in this process, require time-consuming steps for their removal [18].

The spray-drying method has grown in popularity to manufacture respirable particles due to the variety of materials that can be employed with it, and the range of sizes (microparticles) that can be obtained. This technique is a one-step process that produces particles from the atomization of a liquid feed. The droplets from the spray are dried to form solid particles. As shown in Table 1.1, RIF-loaded PLGA microparticles have been successfully produced by this technique [50,59]. However, this particle manufacturing process requires high capital costs, and bulky equipment that is expensive to maintain. Process scale-is still an important challenge with this method. This is rooted in the low thermal efficiency of the system i.e., the large volume of heated air with low or no contact with particles [59].

Electrospray, one of the two popular electrohydrodynamic (EHD) techniques, is a facile, inexpensive fabrication method that uses an electric field gradient to create solid or hollow particles. EHD principles, modes of operation, and instruments for small-scale production are well-established and well described in

the literature (see figure 1.3) [57,58,60–63]. The basic, lab-scale ES system consists of (1) a high voltage power supply, (2) a spinneret, and (3) a grounded collector plate. Electrical forces counter the effect of surface tension of the polymer solution extruded from the spinneret. The net result is the formation of a quasi-conical meniscus at the exit orifice. Typically, from the Taylor cone's apex an electrified liquid jet is ejected and breaks down into droplets. Particles are generally formed depending on where, during the "time of flight" of the electrified droplets to the collector electrode, solidification due to solvent evaporation occurs [57,58,60–63].

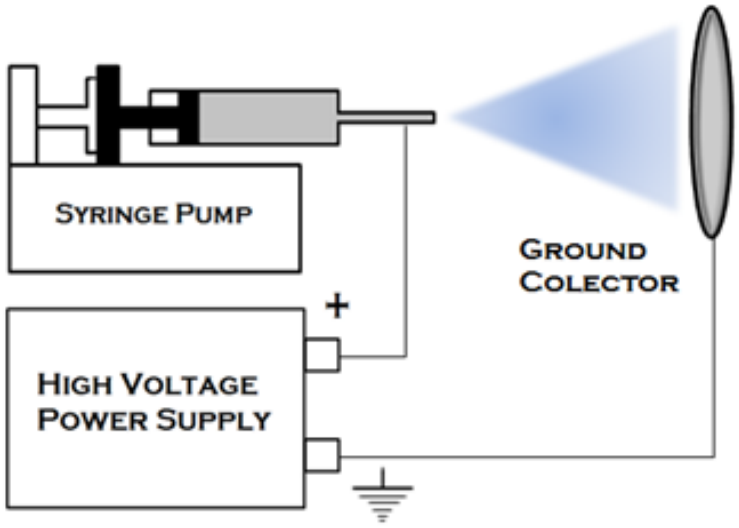

Figure 1.3 - Basic electrospray apparatus

Chakraborty et al. discussed the physics involving electrospray [58]. Important phenomena governing electrospray are electrodynamic, gravity, inertia, and drag forces. Electrodynamic forces are proportional to the induced electric field on the

charged nozzle and flying droplets. Drag forces depend on the jet velocity, and the viscosity of the gas surrounding the nozzle. The following scaling relation has been developed:

$$d = \alpha \frac{Q^{aQ} \varepsilon_0^{a\varepsilon} \rho_1^{a\rho}}{\sigma_1^{a\sigma} \gamma_1^{a\gamma}}, (\text{equation } 1.1)$$

Where, d is droplet diameter, Q is the volume flow rate, ε_0 is the permittivity of free space, ρ_1 is liquid density, σ_1 is liquid surface tension, γ_1 is liquid bulk conductivity, and α is a coefficient that depends on liquid permittivity. These and other characteristic parameters and coefficients have been studied by different authors. Typical values are in table 1.2:

Table 1.2. Coefficient for equation 1.1 to determine droplet size

Authors	aQ	aε	aρ	aσ	aγ
Fernandez de la Mora and Loscertales [64]	1/3	1/3	0	0	1/3
Gañán Calvo [65] and Gañan Calvo et al. [66]	½	1/6	1/6	1/6	1/6
Hartman et al. [67]	½	1/6	1/6	1/6	1/6

Two principal modes of electrospray operation for making ultrafine particles have become popular over the last two decades: monoaxial and coaxial fluid delivery. Monoaxial electrospray utilizes a one-nozzle, one-liquid delivery arrangement, and creates solid particles with matrix-encapsulated drugs. Coaxial electrospray uses an emitter based on two coaxial nozzles to make core-shell particles.

Monoaxial electrospray was used in this dissertation to produce RIF-loaded solid GluN-LLA and PLA nano- and microparticles. In this case, RIF was embedded in the particles through dissolving it in the polymer solution precursor.

The electrospray method has several advantages in the preparation of nano- and microparticles over other methods. Residual charges on the particles and drying effect of EHD “atomization” assure little or no aggregation on solvent evaporation. The absence of high-shear forces such as those present in stirring or sonication protects drugs with fragile molecular structures. Besides high loading levels and high encapsulation efficiency, electrospray achieves uniform dispersion of the drug in the polymeric matrix if so desired. Also, EHD methods are easy operable at a laboratory scale [58].

Thus, among the various ultrafine particle preparation methods currently available [56–58], electrohydrodynamic atomization (EHDA) stands out for its simplicity and general applicability [57,58]. The EHDA production of particles from many synthetic and naturally occurring polymeric systems as drug carriers has been demonstrated in the past [58,61,68]. It has also been shown recently that both particle size and morphology can be controlled in a relatively simple manner with this method [69].

Papers on EHDA processing of polylactides (PLAs) for this particular application are scarce [70], and very few studies reporting on the preparation of MP made from PLA polymers loaded with RIF using spray drying techniques [55,71,72].

Bain and co-workers [71] produced RIF loaded PDLLA microparticles from a series of mixtures of low (2 kDa) and modestly low (9 kDa) molecular weights (MWs). The RIF release rates were strongly affected by relatively small changes in the mixture composition, and increased with increasing content of the low MW (LMW) fraction. Celikkaya and co-workers [72] prepared a series of microparticles using PDLLA with MWs in the 9,7-23 kDa range, obtaining a maximum drug loading of only 10%. Moreover, a rather “permanent” RIF entrapment within the polymer matrix occurred. This, coupled with the slow PDLLA degradation kinetics, resulted in only a 20-30% release of the initial drug payload. Similarly, Coowanitwong and collaborators [73] found incomplete RIF release during the first 24 hours from microparticles prepared using HMW PLA (75-125 kDa) and PLGA (40-65 kDa). It is worth mentioning that among the polylactide polymer family members, PDLLA is favored for drug delivery applications owing to its disordered chain structure, which in turn translates into a purely amorphous material [43].

1.3.1.4. Drug Delivery system: Cost analysis

An efficient delivery vehicle should have the potential to reduce dosages and side effects related to unintended dispersion of the drug through the body. Delivering the correct dosage to the proper location is important not just from safety, convenience and efficacy standpoints, but also from a cost-cutting perspective [74] . The implementation of RIF-loaded GluN-LLA ultrafine particles as drug delivery systems for the treatment of tuberculosis would potentially decrease the conventional therapy costs by reducing the amount of drug used

during the treatment. As mentioned before, the RIF-loaded particles presented in this dissertation are eventually intended to be administrated by the inhalation route, and thus to effectively target the *M. tuberculosis* harboring inside the alveolar macrophages. The immediate significance of this targeting is two-fold: to achieve drug dose reduction, and to potentially decrease the overall treatment time. A reduction in the amount of drug used for adequate treatment would translate into a substantial decrease in costs when compared to conventional treatment modalities. In addition to reduction in the occurrence and frequency of side effects, the fact that GluN-LLA particles deliver RIF for a long period of time (~14 days, chapter 3) would decrease the frequency of drug administration, and as a consequence, patients would likely be more compliant to treatment. High levels of adherence to treatment will also stop the development of MDR tuberculosis (and decrease the use more expensive and toxic drugs), and ultimately reduce healthcare costs.

Even when GluN-LLA synthesis and particle processing are cost-effective and easily scalable when compared with other techniques (section 1.3.1.3), the final drug delivery product, which is envisioned as dry powder inhaler, will eventually cost more than pure RIF on a weight of drug basis. However, the cost cutting factors in this case will be efficacy enhancements, patience compliance and shorter treatment duration [75]. In this regard *Owens et al.* published an evaluation of the cost-effectiveness of a novel first-line treatment with hypothetical regimens of equal efficacy, higher cost, and shorter duration than the

conventional 6 months treatment. In their study, these authors conclude that the more novel treatment approach effectively reduced treatment costs.

This doctoral dissertation proposes a pulmonary RIF delivery system capable to cure tuberculosis and effectively reduce the cost of treatment. This hypothesis would ultimately have to be tested by a comprehensive cost-effectiveness study.

1.3.2. Glucosamine L-lactide (GluN-LLA)

GluN-LLA, a new biocompatible oligomer is produced by a 'one-spot' synthesis route, where L-lactide chains are grown onto glucosamine molecules via –OH groups. This polymer and the production method were designed and first characterized by *Skotak and Larsen* [1] at the University of Nebraska – Lincoln in 2010. These authors thoroughly characterized this polymer system via ^{1}H and ^{13}C nuclear magnetic resonance (NMR), Fourier transform infrared (FTIR), and UV-visible spectroscopies, electrospray ionization mass spectrometry (ESI-MS), gel permeation chromatography (GPC), and differential scanning calorimetry (DSC). Conveniently, this polymerization method does not employ the conventional organometallic tin catalyst for the lactone ring-opening polymerization process, which eliminates the presence of cytotoxic impurities in the product. The synthesis of L-lactide grafted chitosan [2] was also successfully achieved by using this methodology, which demonstrates the simplicity and flexibility for grafting lactone chains onto simple aminosugars and sugar rings.

GluN-LLA (figure 1.2) is a low molecular weight star-shaped biocompatible and biodegradable polymer. By controlling the initial LLA-to-core molecule molar ratios it is possible to control the length of the lactide substituents, and consequently this GluN-LLA holds the capability of having a tunable hydrophobicity-hydrophilicity balance. In this dissertation, GluN-LLA 1:32 with a degree of substitution of 3.8/4 and lactate side length of ~11 monomers was used to produce RIF-loaded and drug-free nano- and microparticles (Table 1 in ref [1]).

The fact that the building blocks of two of the most well-known biocompatible polymers (chitosan and PLA) have been used to produce one LMW co-polymer, a priori positions GluN-LLA as a potential material for biomedical applications. Moreover, the hypotheses of biocompatibility and biodegradability are tested in this dissertation. This thesis is thus the first documented implementation of a GluN-LLA oligomer as drug delivery system in particular, and biomedical applications in general. In this work, biocompatibility of the GluN-LLA nano- and microparticles is assessed via cell viability in Chapter 3.

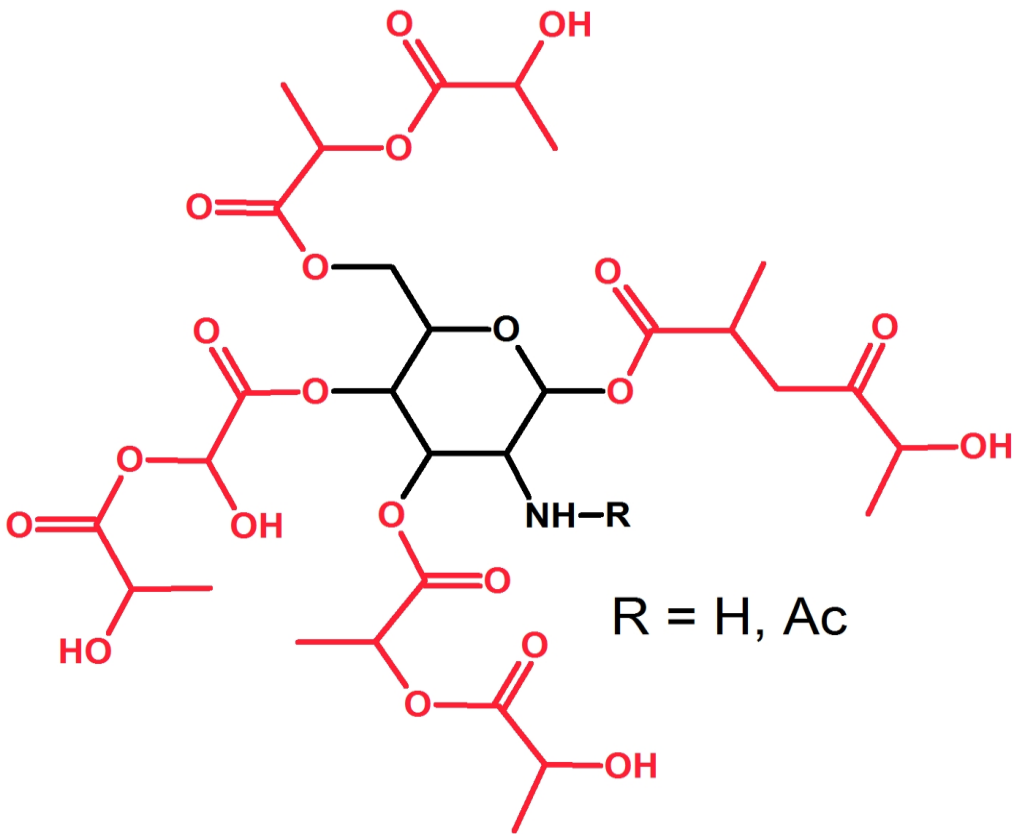

Figure 1.2. Glucosamine-L-lactide oligomer

1.3.3. Antimicrobial Susceptibility Test

Antimicrobial susceptibility testing is important to determine susceptibility of species that are considered clinically significant in antimicrobial agents, or to detect resistance in individual bacterial isolates. The Clinical and Laboratory Standards Institute (CLSI) develops and provides standardized methods to perform antimicrobial susceptibility tests for several groups of bacteria. For instance, CLSI recommends the standard broth microdilution method for M. Smegmatis, thesis's tuberculosis-model bacteria.

The broth microdilution method is based in the ability of the isolate (bacteria suspension) to grow in broth containing a single antibiotic concentration. The critical minimum concentration of an antimicrobial agent that prevents bacteria growth represents the minimum inhibitory concentration (MIC) [76,77]. Briefly, known quantity of bacteria is exposed to specified concentrations of one antibiotic. Following overnight incubation, visible bacterial growth (as evidenced by turbidity) is examined, and MIC is determined [78]. Using these standards, the minimum bactericidal concentration (MBC), which is the lowest concentration of the drug that kills ~99.9% of bacteria, can be determined.

1.4. Approach: Ultrafine Particles as Drug Delivery System

Many treatment strategies to increase the dose of antibiotics inside alveolar macrophages have been devised in recent years. Among them, drug encapsulation in liposomes, nanoparticles (NP) or microparticles (MP) that can undergo endocytosis by alveolar macrophages holds significant promise [15,40,53,79,80]. Some advantages of using encapsulated drugs for infection treatments are shortened treatment time, reduced dose frequency, and lower doses [81]. In addition, by using drug-loaded particle systems the intracellular delivery and bactericidal activity of antibiotics have shown significant improvement when compared to that of the free drug [53,82–84].

Particles can be delivered by several administration routes, including inhalation. One important benefit of the inhalation route for tuberculosis treatment is that the

drug would be released to the desired site, directly to the alveolar macrophages where *M. tuberculosis* is harboring. This would facilitate a faster antimicrobial action, and help to reduce the long period of the current treatment. The main advantage of the inhalation route resides in the fact that it eludes first-pass metabolism, thereby reducing side effects, lowering drug dose, and more efficiently targeting alveolar macrophages [6,85]. High intake of RIF could present serious hepatic side effects, such as hepatotoxicity and renal failure [13]. Thus, in this work, the development of a particulate system able to efficiently deliver the right drug amounts over time to alveolar macrophages is sought. The RIF-loaded particulate system is envisioned as a pulmonary delivery of RIF.

CHAPTER 2
Materials and Methods

CHAPTER 2: Materials and Methods

2.1. Materials 35

2.1.1 Polymer synthesis 35

2.2. Particle preparation and characterization 36

2.2.1 Particle preparation 36

2.2.2 Size and morphology 37

2.2.3. Drug release studies 38

2.2.4 Particle degradation 38

2.2.5 Drug encapsulation efficiency 39

2.2.6. Thermal properties of RIF loaded particles 40

2.3 Data fitting and statistical analysis 40

2.4 Evaluation of particle effects on bacteria 41

2.4.1 Bacterial strain 41

2.4.2 Particle toxicity on M. smegmatis 41

2.4.3 Determination of minimum inhibitory concentration (MIC) 42

2.5 Evaluation of particle loading effects on macrophages 43

2.5.1 Cell line 43

2.5.2 Cytotoxicity of particles on macrophage cells 43

2.5.3 Particle uptake, and intracellular localization by confocal microscopy 44

2.5.4 Intracellular killing of M. smegmatis 44

2.1. Materials

Rifampicin (RIF, >97% HPLC), D-(+)-Glucosamine hydrochloride (GluN-HCl, min. 99%), ethyl acetate (99.8%) and methanesulfonic acid (>99.5%) were from Sigma-Aldrich, and ethanol (>99.5%) was received from McCormick Distilling Co., Inc.. High molecular weight poly-L-lactide (HMW PLA, NatureWorks Ingeo™ 8302D) with M_n = 123 kDa and polydispersity (PDI) 1.75 (GPC)) was purchased from Jamplast, Inc. The L-lactide (LLA, 98%, Alfa) was re-crystallized from toluene, vacuum-filtered in an argon atmosphere, vacuum-dried, and stored in a desiccator. All the other chemicals and reagents were purchased from Sigma-Aldrich except where indicated. The low molecular weight poly-L-lactide and GluN-LLA polymer synthesis is described in the next section.

2.1.1 Polymer Synthesis

Low molecular weight poly-L-lactide (LMW PLA, M_n = 2,500 Da, PDI=1.4 (GPC)) was synthesized according to a procedure published elsewhere [86]. The GluN-LLA (M_n = 3,100 Da (NMR), PDI = 1.47 (GPC)) with average side-chain length of 11 monomeric L-lactide units, was prepared according to a procedure reported earlier [1,2]. Briefly, 10 mL of methanesulfonic acid were transferred into a 50 mL flask under argon atmosphere and placed in an oil bath kept at 40°C. Subsequently, 3.5 mmol of GluN-HCl was added and stirred until homogenization. Then, the L-lactide was added to the reaction mixture, and the flask was flushed with argon for 10 minutes to remove the liberated gaseous HCl.

Polymerization of L-lactide occurred for four hours, and the reacting mixture was afterwards quenched with an acid-base neutralization solution, as described elsewhere [2]. Vacuum filtration and vacuum drying overnight at the ambient temperature were carried out to isolate and dry the product. Samples were stored in a desiccator until use.

2.2. Particle Preparation and Characterization

2.2.1 Particle Preparation

Polymeric nanoparticles were prepared from a 5% (w/v) GluN-LLA or LMW PLA, while microparticles were prepared from a 20% (w/v) GluN-LLA or 1% (w/v) HMW PLA. The preparation of polymeric precursor solutions was done by dissolving the corresponding polymers into ethyl acetate. These solutions were processed into four different sets of particles using a conventional single-nozzle EHDA setup. The resulting particles were labeled as SMP-GluN-LLA, SMP-LLA and MP-GluN-LLA, MP-LLA, respectively. For the preparation of RIF-loaded particles, three different drug loadings were used: 10, 20 and 50 wt%, which correspond to RIF-to-polymer mass ratios of 1:10, 1:5 and 1:1, respectively, being the 1:5 and 1:1 ratios the most studied in the present thesis. The precursor solution was loaded into a Hamilton series 1000 gastight syringe (model 1001, 1 mL), then a 19 gauge, blunt needle was attached to the syringe (to serve as the EHDA nozzle). Subsequently, the syringe was attached to a digital syringe pump (Cole-Parmer 74900-00, Vernon Hills, IL). Voltage differences in the range of 5-

15 kV, (Gamma High Voltage Research ES30P-5W/PRG, Ormond Beach, FL) and a nozzle-to-collector distance of 10 cm were used in the course of a typical experiment. Various flow rates in the range of 0.2-0.5 mL h^{-1} were tested to find optimal processing conditions in order to make particles with narrow diameter distributions. The particles were deposited onto an aluminum foil collector tightly wrapped around 15 cm OD circular copper disk. The temperature and relative humidity during the collection of particles were approximately 24ºC and 45%, respectively. The collection time was limited to 10 minutes (optimization phase) or extended up to a few days to collect amounts of particles suitable for further studies.

2.2.2 Size and Morphology

Particle size and morphology were assessed via scanning electron microscopy (SEM), using a Hitachi S-3000N microscope with an accelerating voltage of 15 kV and working distance of approximately 10 mm. Coating with metallic gold for 2 minutes before SEM characterization was used to enhance the contrast of non-conducting samples. The electrical current inside the chamber of the Technics Hummer II sputter coater was kept constant (10 mA). Statistical analysis of particle size measurements from SEM images was performed on sets of at least 250 counts within each specimen.

2.2.3. Drug Release Studies

Drug release studies were performed under “perfect sink” conditions [26]. Briefly, a mass equal to 50 mg of RIF-loaded particles was dispersed in 5 mL of phosphate buffered saline (PBS) (n=3) (pH = 7.4) supplemented with 0.02% of ascorbic acid as an antioxidant [40], the vials were kept in a thermostat/shaker at 37.0±0.1°C in the dark. Samples of 200 µl were extracted from each vial every hour for the first 8 hours, and then every 24 hours. The total volume was kept constant by replacing the extracted sample volume with 200 µl of fresh PBS. RIF content was measured with a Beckman DU-640 spectrophotometer in the 250-550 nm wavelength range. In the past, the RIF release kinetics had been evaluated at the isosbestic point of the drug, and through its quinone degradation product (330 nm) [38,71]. Absorbance values at 310 nm were used to calculate the concentration of RIF in the absence of drug oxidation, which was prevented by addition of ascorbic acid and a lack of sample exposure to light.

2.2.4 Particle Degradation

Polymer degradation studies were performed using a modified PBS (pH = 7.4) solution: water was replaced with deuterated water to facilitate NMR analysis of the released L-lactic acid. First, the pH of the PBS stock solution was adjusted to 7.4 with 1 M HCl, then water was evaporated and the remaining solid was dried under vacuum. Then, the dry PBS powder was dissolved in deuterated water

(D2O, 99.8 atom % D, Cambridge Isotope Laboratories) for further use. Solid polymeric particles (50 mg) were dispersed in 5.0 mL of deuterated PBS and the suspension was kept in the dark at 37 °C while shaking it. For NMR analysis, 0.5 mL aliquots were drawn every 24 hours and ^{1}H NMR spectra were recorded on a Bruker Avance 500 NMR spectrometer at 500.13 MHz to track the release of L-lactic acid. Following analysis, samples were poured back into their respective particle suspensions. These studies were done in triplicate for all tested particle types, and for 14 consecutive days.

2.2.5 Drug Encapsulation Efficiency

Approximately 40-50 mg of RIF loaded particles were treated with 5 mL of anhydrous ethanol for 10 minutes (L-lactide polymers are not soluble in this solvent, RIF solubility in ethanol is roughly 10 mg/mL). The suspension was then centrifuged, the supernatant transferred to a 30 mL beaker and subsequently diluted to 15 mL. UV-Vis spectra of RIF in ethanol were recorded in the 250-550 nm range, and concentrations were calculated based on the absorption peak at 306 nm.

The drug content entrapped within the particles was analyzed with ^{1}H NMR spectroscopy, using deuterated chloroform ($CDCl_3$, 99.8 atom % D, Sigma-Aldrich) as solvent. Characteristic signals of methyl groups of RIF (1.04, 0.89 and 0.62 ppm) and polymer matrices (1.60 ppm) were compared and used to

calculate the drug-to-polymer ratio. Particles that were not treated with ethanol were used as reference.

2.2.6. Thermal Properties of RIF Loaded Particles

Differential Scanning Calorimetry (DSC) runs were performed on Q100 machine (TA Instruments, New Castle, USA), calibrated for temperature and heat flow using indium (melting point 156.6 °C and ΔH_m, 28.45 J/g, respectively). Two analytical runs (to confirm repeatability) were performed on each sample at a heating rate of 10°C/min., by ramping temperature from 0 to 300°C, and the sample compartment was flushed with dry nitrogen flowing at 25 mL/min. An empty hermetic aluminum pan was used as a reference.

2.3 Data Fitting and Statistical Analysis

Data fitting of temporal RIF release profiles was performed using non-linear curve fitting built-in module of the Origin® 9.0 software. Typically, 60% of the data points were used and fitted to the Korsmeyer-Peppas equation (as required by the model) [26]. Statistical evaluation was performed using ANOVA test with p-values below 0.05 and 0.01 considered as significant.

2.4 Evaluation of Particle Effects on Bacteria

2.4.1 Bacterial Strain

M. smegmatis ATCC 607 was purchased from Hardy Diagnostics (Santa Maria, CA), and cultured at 37ºC and 150 rpm in Difco Middlebrook 7H9 (BD Diagnostics, Sparks, MD) medium supplemented with 0.5% (v/v) glycerol and 0.05% Tween 80 to prevent clumping, 10 µg/mL cycloheximide to prevent fungal contamination, 50 µg/mL carbenicillin to prevent other bacterial contamination, and ADS (0.5% bovine serum albumin, 0.01 M dextrose and 0.015 M NaCl). For each experiment, a fresh overnight culture was prepared with a terminal OD600 reading less than 0.4.

2.4.2 Particle Toxicity on M. Smegmatis

Three million colony forming units (cfu) of freshly prepared mycobacteria were inoculated in 10 mL of 7H9 complete medium for 1 hour at 37ºC before the addition of different amounts of particles (0, 300, 600 and 1,200 µg/mL). The cultures were maintained in the oven at 37ºC with continuous shaking at 150 rpm for 24 hours, and then 10 µL of culture was inoculated onto 7H10 agar plates (7H10 agar supplemented with the same ingredients as 7H9 complete medium without Tween 80) without spreading out, and incubated at 37°C for 3 days to produce visible colonies. Mycobacteria in 7H9 complete medium without particles were considered the particle toxicity control. Pictures of agar plates were taken

with a digital camera (24 Mega Pixels resolution); areas of the colonies formed were quantified by ImageJ software.

2.4.3 Determination of Minimum Inhibitory Concentration (MIC)

The MIC of free RIF and RIF-loaded particles for *M. smegmatis* were determined by standard macrobroth dilution techniques recommended by the Clinical and Laboratory Standard Institute (CLSI). Briefly, a series of dilutions of RIF-free (0, 1, 2, 4, 8, 16, 32, 64, 128, 256, 512 µg/mL) and encapsulated RIF particles (according to 1:5 RIF-to-polymer mass ratio, 0, 5, 10, 20, 40, 80, 160, 320, 640, 1280, 2560 µg of loaded particles/mL, and 1:1 ratio 0, 2, 4, 8, 16, 32, 64, 128, 256, 512, 1024 µg of loaded particles/mL) in 7H9 medium were prepared. Bacterial suspensions were then added to each tube to make final inocula of 3 x 10^5 cfu/mL; the lowest concentrations in antibiotic formulations that inhibited the visible bacterial growth after 24 hours were assigned as MIC using McFarland turbidity standard value of 0.5 as reference. 10 µL of culture from each tube was taken and then placed onto a 7H10 agar plate without spreading it out. The plates were cultured at 37^{o}C for 3 days before the colonies were analysed. Minimum bactericidal concentration (MBC) was defined as the smallest concentration which kills at least 99.9% of bacterial population compared with those in control vials.

2.5 Evaluation of Particle Loading Effects on Macrophages

2.5.1 Cell Line

Mouse macrophage cell line J774A.1 was purchased from ATCC (Manassas, VA). The cells were grown in Dubelco's modified eagle's medium (DMEM, Global Cell Solutions, Charlottesville, VA) supplemented with 10% fetal bovine serum (FBS, PAA Lab, Westborough, MA) and antibiotics containing 100 units/mL penicillin, 100 µg/mL streptomycin and 250 ng/mL amphotericin B (Lonza, Walkersville, MD) at 37^{o}C and 5% CO_2 in a humidified incubator.

2.5.2 Cytotoxicity of particles on macrophage cells

WST-8 assay (Dojindo Molecular Technologies, Inc) was performed per manufacturer's instructions. In brief, J774A.1 macrophages were seeded in 96-well plates at a density of 1 x 10^4 cells/well, and incubated with SMP-GluN-LLA, MP-GluN-LLA, SMP-LLA, and MP-LLA (0 (control), 30, 60, 120 and 240 µg/mL) for 3 days at 37°C in humidified atmosphere (90% humidity), 5% CO_2. WST-8 reagent solution (10 µL) was added to each well without changing medium, and the plates were incubated for 1 hour prior to OD450 measurement with a BioTek Elx800 microplate reader. Viability of J774A.1 cells was determined from the absorbance of WST-8 in the cell suspension and sample without particle exposure was taken as 100% viability.

2.5.3 Particle Uptake, and Intracellular Localization by Confocal Microscopy

To determine the internalization of particles into macrophages, 4 x 10^5 cells were seeded in 35mm glass bottom dishes (MatTek, Ashland, MA) and incubated for 48 hours with 120 µg/mL particles labelled with 1 % poly-caprolactone-fluorescein conjugate (PCL-fluorescein, Advanced Polymer Inc, Carlstadt, NJ). For these experiments, 1 % w/w PCL-fluorescein/polymer was added to the GluN-LLA or PLA solution before particle fabrication. Subsequently, the cells were stained with 100 nM of MitoTracker® or LysoTracker® (Invitrogen, Carlsbad, CA) in serum-free and phenol red-free DMEM for 10 minutes. CellMask™ plasma membrane staining (Invitrogen) was also performed to confirm the particle internalization. Finally, cells were washed and visualized with a confocal microscope (Olympus FV500-IX 81).

2.5.4 Intracellular Killing of M. Smegmatis

To examine the effects of RIF loaded particles on killing efficiency of *M. smegmatis* in macrophages, 10^5 cells per well were seeded in 24-well plates and allowed to grow for 24 hours before infection. After washing with antibiotics-free medium twice, 20 multiplicity of infection (MOI: ratio of bacteria/cells) of fresh growing *M. smegmatis* was used to infect the cells for 1 hour and then extracellular bacteria were killed by the addition of gentamicin (20 µg/mL). Free (30 µg/mL), or RIF loaded particles (60 µg/mL, according to 1:1 RIF-to-polymer mass ratio), was then loaded into the cell culture with growing medium without

antibiotics. After the incubation period, cells were washed and lysed with water and intracellular survival was estimated by plating serially diluted cultures on 7H10 plates. Pictures of agar plates were taken with a digital camera (24 MP resolution), and the colonies were counted after 3 days with ImageJ software. To determine the relative population of surviving cells after infection, macrophages were stained with the Live/Dead viability kit (Invitrogen, 4 μM EthD-1 and 2 μM Calcein AM) before lysed. After 10 minutes of incubation with dyes, cells were examined with VWR Vistavision Inverted Epifluorescence microscope attaching to a LissView Imaging system. Live cells were counted with ImageJ software.

CHAPTER 3

Results and Discussion

CHAPTER 3: Results and Discussion

CONTENTS

3.1. Particle fabrication: optimization of processing conditions 48

3.2. Fabrication of pure, and RIF-loaded submicron- and micron-sized particles 52

3.3. Drug entrapment efficiency 59

3.5. Particle degradation and thermal properties: impact on drug release kinetics 66

3.6. Particle toxicity on M. smegmatis 71

3.7. Minimum inhibitory concentration (MIC) and minimum bactericidal concentration (MBC) of free RIF and RIF loaded particles 74

3.8. Cytotoxicity of particles on macrophage cells 77

3.9. Intracellular localization of particles by confocal microscopy 79

3.10. Intracellular killing of M. smegmatis 84

3.1. Particle Fabrication: Optimization of Processing Conditions

The electrospray technique was used to prepare four sets of particles composed of two different polymeric materials, GluN-LLA and PLA. These groups of particles were labeled as SMP-GluN-LLA, MP-GluN-LLA, SMP-LLA, and MP-LLA. In order to determine the optimal conditions for particle production, electrospray variables such as polymer concentration, voltage, tip-to-collector distance and flow rate were varied (section 1.3.1.3). Due to the fact that ultimately, fully biocompatible drug delivery systems are desired, particles were prepared using (the relatively less toxic) ethyl acetate solvent to dissolve GluN-LLA and PLA polymers. An experimental setup similar to the one illustrated in Figure 1.3 was employed to produce the particles. Particle size and morphology was characterized by the processing of SEM images with Gimp 2.8 software. It was determined that the simplest way to achieve particle size control was by varying polymer concentration. Preliminary tests using the GluN-LLA oligomer were performed at three different weight/volume percentages: 5, 10 and 15 (Fig. 3.1), while keeping flow rate in all cases at 0.5 mL/h. It is clear that at 5 kV, average particle diameters increase (0.79, 0.91 and 2.62 μm) with increasing polymer concentration, and that the particle size distributions (PSDs) were relatively broad in all samples (standard deviation: 0.94, 1.01, and 1.88, respectively). Increasing the processing voltage to 10 kV resulted in decreased average particle diameters (Fig. 3.1B).

The polymer concentration was then fixed at 5 %, and the flow rate was varied from 0.2 to 0.5 mL/h, in 0.1 mL/h increments (Fig. 3.2). As it turned out, samples processed at 5 kV displayed a bimodal PSD, with 80% of particles being in the submicron region (Fig. 3.1, inset). This is normally indicative of either the presence of more than one mode of electrified jet breakup, or the occurrence of a “satellite” droplet formation mechanism [87]. At 10 kV, a practical PSD unimodality was achieved at a flow rate of 0.3 mL/h, with only 3% of population consisting of supramicron-sized particles. However, a tradeoff between unimodality and particle diameter (if the general goal of using EHDA is indeed making ultrafine particles) becomes apparent, as the former comes at the expense of making larger particles (Fig. 3.2B).

Since in this dissertation, one objective was to focus on drug release from well-defined PSDs, it was preferred to process the samples at a flow rate 0.3 mL/h and voltage of 10 kV. Interestingly, increasing the voltage to 15 kV did not lead to smaller particle diameters. This effect is attributed to a multi-jetting mode being in operation exclusively at 10 kV. The single-jet mode was observed at 5 and 15 kV. The latter normally leads to larger particles relative to cases in which more than one electrified liquid jet is ejected from the Taylor cone. This same trend was also observed during the attempts to optimize the microparticle design from GluN-LLA and HMW PLA, which suggests that this may be a characteristic of the solvent system, rather than a solute effect.

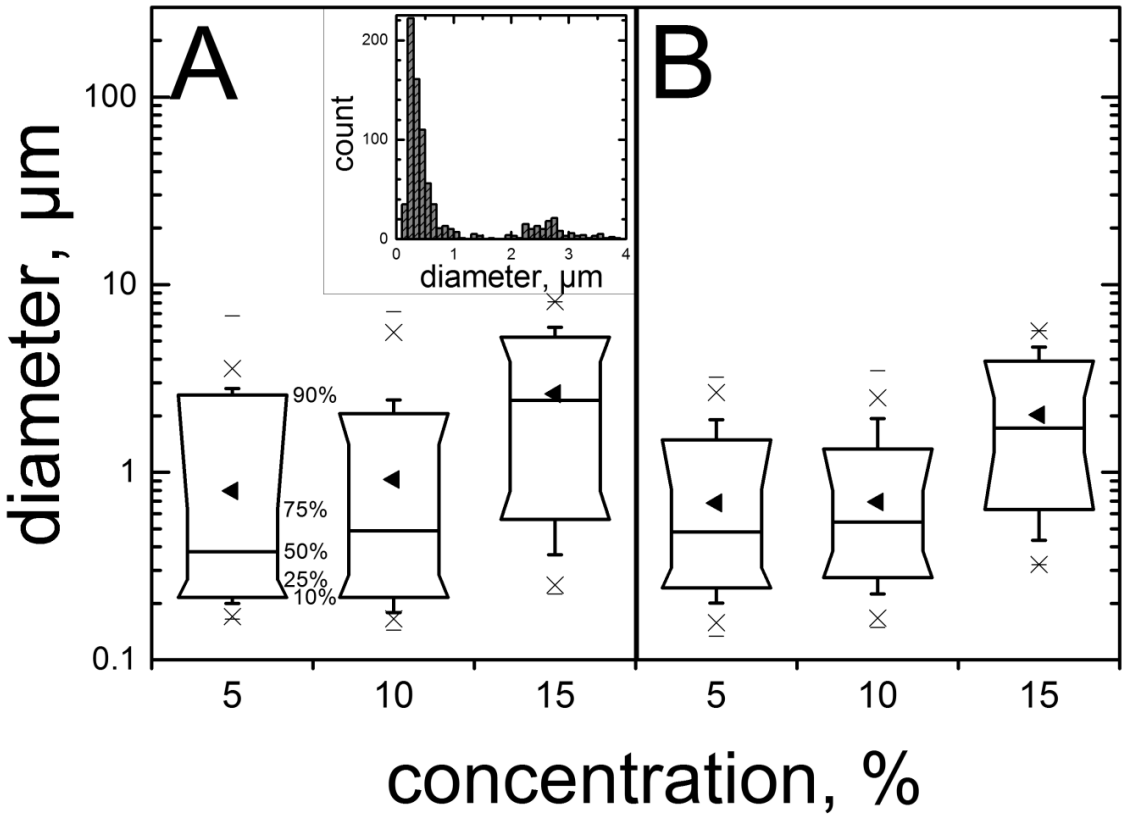

Figure 3.1. Control over particle size is achieved by varying the concentration of GluN-LLA. Samples were solubilized in ethyl acetate and processed at 0.5 mL/h flow rate and voltages of: A) 5 kV, B) 10 kV. With increasing voltage, the average particle size decreases while particle diameter distribution becomes narrower. Increasing polymer concentration increases the average particle size (◄). Box range: 10-90%, whisker range: 5-95%, (x) 1-99%, (−) min. and max. values of particle diameter within investigated population. Inset: bimodal particle size distribution for sample prepared using 5 % w/v GluN-LLA concentration. Particle diameter means are significantly different ($p<0.01$) at 5kV and 10kV.

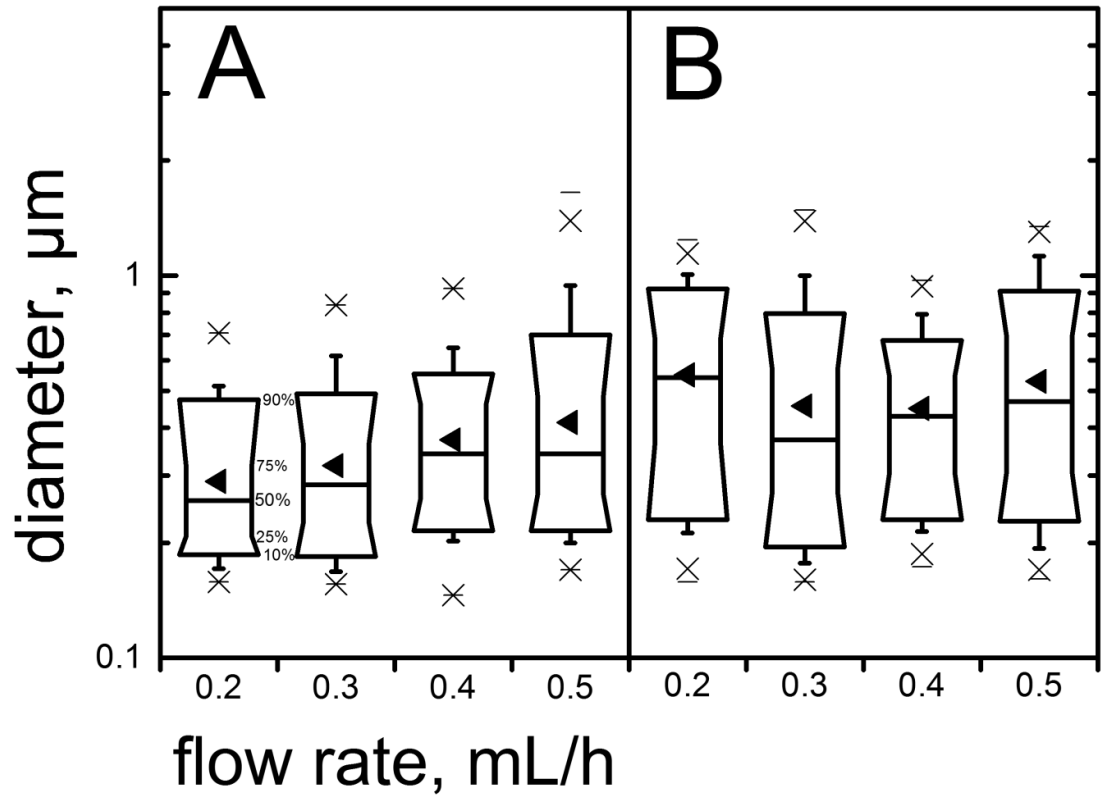

Figure 3.2. The effect of processing conditions, flow rate and voltage (A: 5 kV, B: 10 kV) on particle size and distribution. Particles were prepared using a 5% (w/v) solution of GluN-LLA in ethyl acetate. Processing at 5 kV resulted in a bimodal particle size distribution with 80% of the population in sub-micrometer range. Box range: 10-90%, whisker range: 5-95%, (x) 1-99%, (−) min. and max. values of particle diameter within investigated population Box plots present submicron populations exclusively. Particle diameter means are significantly different ($p<0.01$) at 5kV and 10kV.

3.2. Fabrication of Pure, and RIF-loaded Submicron- and Micron-sized Particles

The main objective of the *in vitro* drug release studies was to gain some insight into the difference in behavior between the GluN-LLA and a broadly accepted benchmark, LLA. Submicron particles based on LMW PLA (SMP-LLA) were prepared from their 5% (w/v) solutions in ethyl acetate at the chosen processing conditions (0.3 mL/h, 10 kV, 10 cm). In order to guarantee complete polymer dissolution and avoid precipitation, the solution needed to remain at 40°C during processing. The average particle diameter is somewhat smaller than those of their branched counterparts (Table 3.1).

For the preparation of MP-LLA, a concentration of 1% (w/v) of HMW PLA was found to be very close to the polymer's solubility. Thus, this value was selected for sample production under the same processing conditions. The MP-LLA in this case were characterized by a toroidal shape (Fig. 3.3) which, based on gained experience, is typically indicative of rapid solvent evaporation leading to imploded "doughnut"- or "raisin"-shaped particles. On the other hand, virtually perfect spherical MP-GluN-LLA are obtained with 20% (w/v) of GluN-LLA in ethyl acetate when processed at a flow rate (Q) of 0.5 mL/h, voltage (V) of 10 kV, and electrode-to-electrode distance (d) of 10 cm electrode-to-electrode distance (Fig. 1.3 and Fig. 3.3). For the preparation of SMP-GluN-LLA, a 5% (w/v) GluN-LLA in ethyl acetate solution was used, which was processed under the same EHDA conditions as their SMP-LLA counterpart (Q = 0.3 mL/h, V = 10 kV, do = 10 cm).

The size and shape of the particles are crucial factors for delivery into the pulmonary airways: particles with aerodynamic diameters between 1-5 μm are preferred [49,88]. Particles with sizes larger than 5 μm are usually deposited in the oral cavity, and particles smaller than <0.5 μm move by Brownian motion and settle slowly. Nanoparticles (<100 nm) are not likely to deposit effectively in the pulmonary airways because they are exhaled before deposition [49]. In this work, two size ranges were intentionally made: SMP between 0.5 to 0.8 μm and MP between 2 to 3 μm. In the past, equipment modifications to the EHDA system were found to be necessary for particle micro-sizing i.e., to extract a fraction of nearly monodisperse PLGA microparticles *in situ*, at the expense of a decreased process efficiency [38]. In this dissertation, nearly monodisperse microparticles were prepared without using any EHDA apparatus modification, and the particle diameter ranges achieved fall within the targeted size ranges for the intended drug delivery long-term application i.e., inhalation.

Table 3.1. Polymers used in RIF release studies. Type, molecular weight (M_n), processing solution concentrations and diameters (average ± SD) of pure and RIF-loaded particles are presented. Voltage: 10 kV, and flow rate: 0.3 mL/h were used unless specified otherwise

Polymer	Molecular weight, Da	Concentration, %	Particle diameter, μm			
			Particle type[c]	Pure polymer	1:5[a]	1:1[a]
GluN-LLA	3,100	5.0	SMP-GluN-LLA	0.50±0.30	0.57±0.45	0.90±0.70
		20.0[b]	MP-GluN-LLA	2.10±0.60	–	–
LMW PLA	2,500	5.0	SMP-LLA	0.37±0.30	0.87±0.80	1.22±1.0
HMW PLA	123,000	1.0	MP-LLA	2.90±0.90	–	–

a) RIF-to-polymer mass ratio used to prepare particles, i.e. 20% and 50% by weight, respectively.

b) Flow rate 0.5 mL/h was used.

c) SMP: submicron particles, MP: microparticles

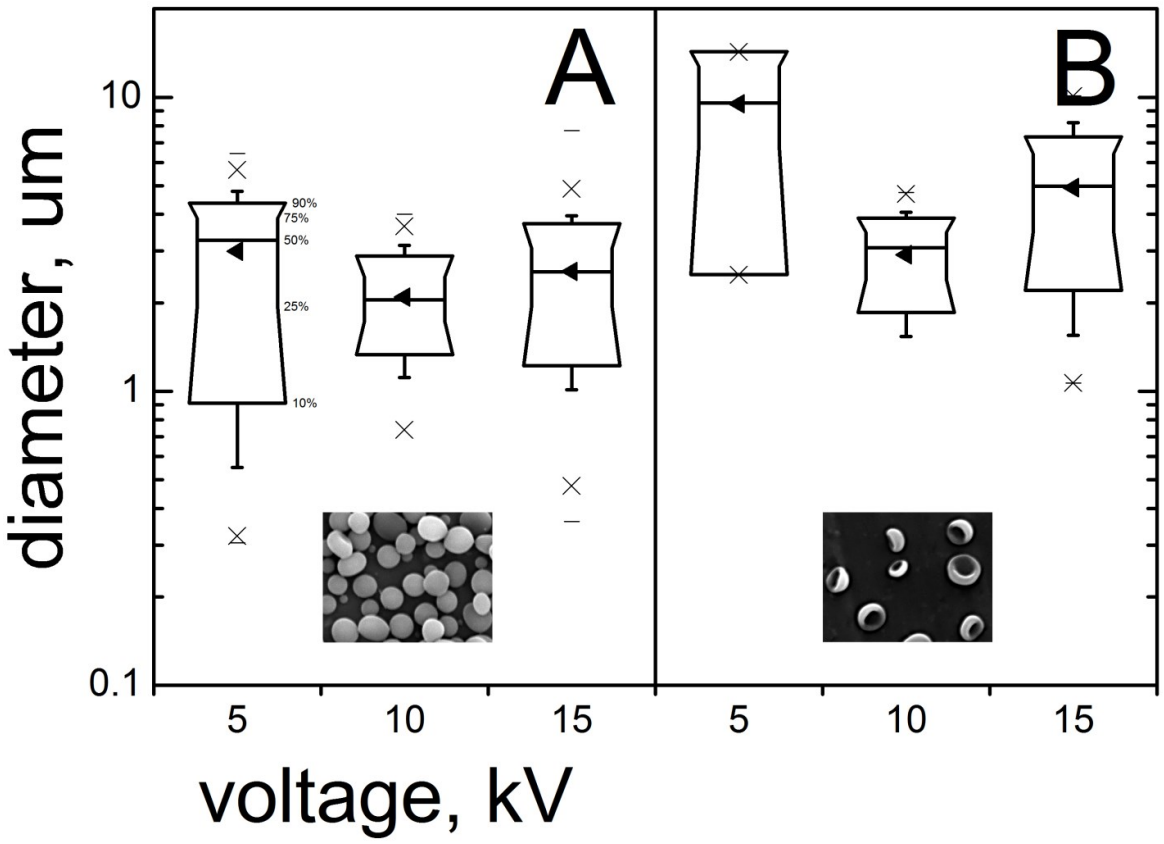

Figure 3.3. MP-GluN-LLA (A) and MP-LLA (B) were prepared at discrete voltages as indicated in respective plots. There are statistically significant differences between all populations within the subsets A and B ($p < 0.01$). Insets show the difference in particle morphology between low and high molecular weight polymers prepared at 10 kV. Spherical MP-GluN-LLA resulted from processing 20% (w/v) GluN-LLA (A). MP-LLA with toroidal shape were obtained by using 1% (w/v) HMW PLA (B). Average particle size (◄), box range: 10-90%, whisker range: 5-95%, (x) 1-99%, (−) min. and max. values of particle diameter within investigated population.

To evaluate the effect of drug loading on particle morphology (Fig. 3.4) and their PSD (Fig. 3.5), tests were performed for SMP-GluN-LLA and SMP-LLA at two drug loadings, namely 20 and 50 wt%, which correspond to RIF-to-polymer mass ratios of 1:5 and 1:1, respectively (Fig. 3.4). It has been mentioned that very high drug loadings and slow release profiles are two extremely desirable traits, and this is exactly the reason why attention has been aimed on such high RIF payloads.

At 20 wt% loading, the broadening of the PSD in this sample (5/1, SMP-LLA) and that of the control differ in a statistically significant manner (*$p<0.01$), but this was not observed in the SMP-GluN-LLA sample, as shown in Figure 3.5 panels A and B. A loading of 50 wt% (5/5) resulted in further particle diameter increases, and in broadening of the PSDs, which could be a consequence of the higher concentration of polymer in the precursor solution. Differences in the particle diameters of SMP-LLA and SMP-GluN-LLA were found to be statistically significant at **$p<0.01$. An increased occurrence of general surface irregularities have previously been observed (e.g., particles with wrinkled surfaces) in PLGA microparticles with increasing RIF loading [38]. It is note however, that this is not indicative of phase separation: in this work case, separate RIF crystals were never observed by SEM.

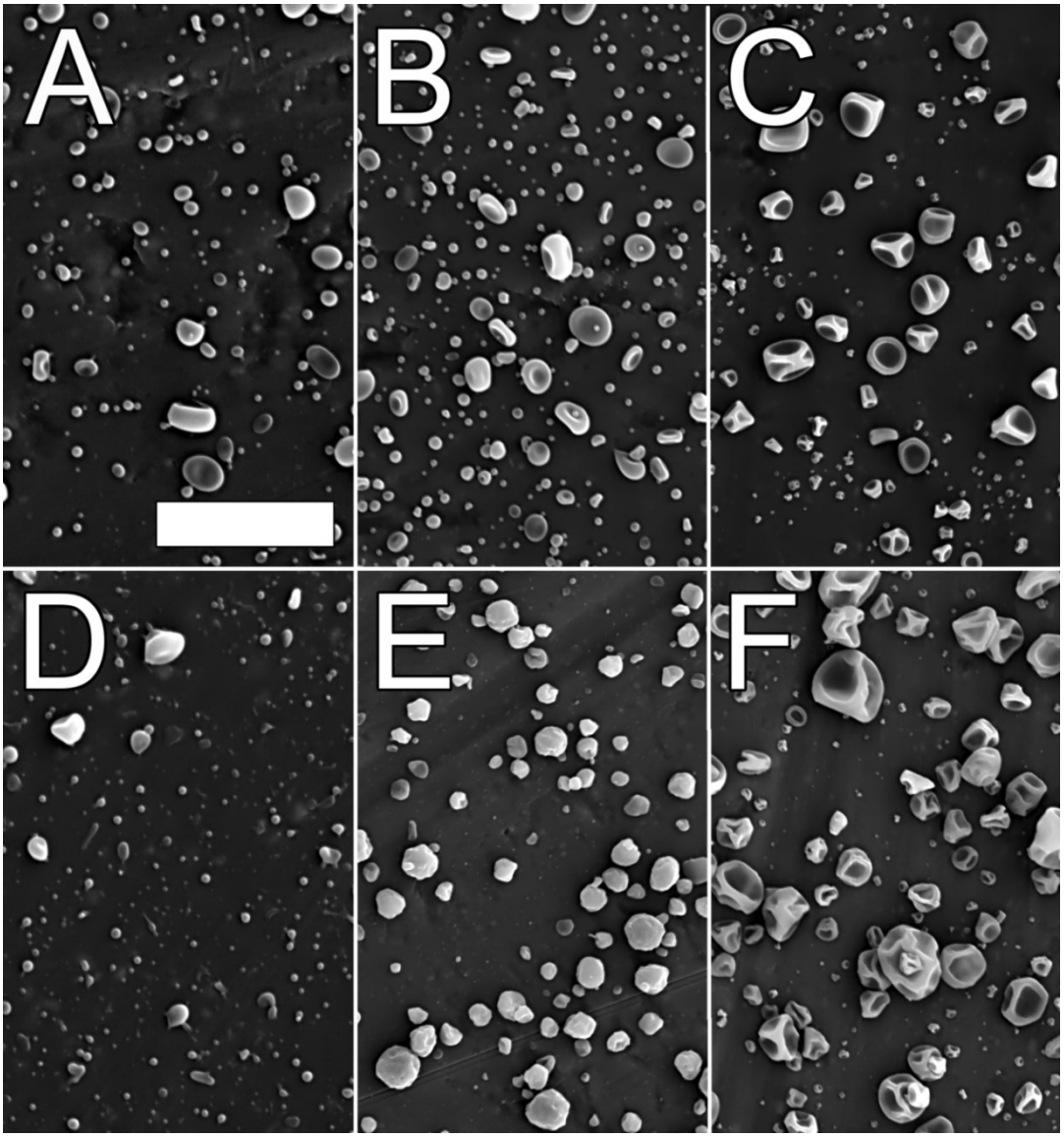

Figure 3.4. SEM images illustrating the gradually changing morphology of polymeric submicronparticles made of low molecular weight polymers as RIF content is increased: SMP- GluN-LLA (top row) and SMP-LLA (bottom row). Pure polymeric particles (A, D) and with RIF-to-polymer mass ratios of 1:5 (B, E) and 1:1 (C, F) are presented. The scale bar (10 μm) is the same for all images, except E (25 μm).

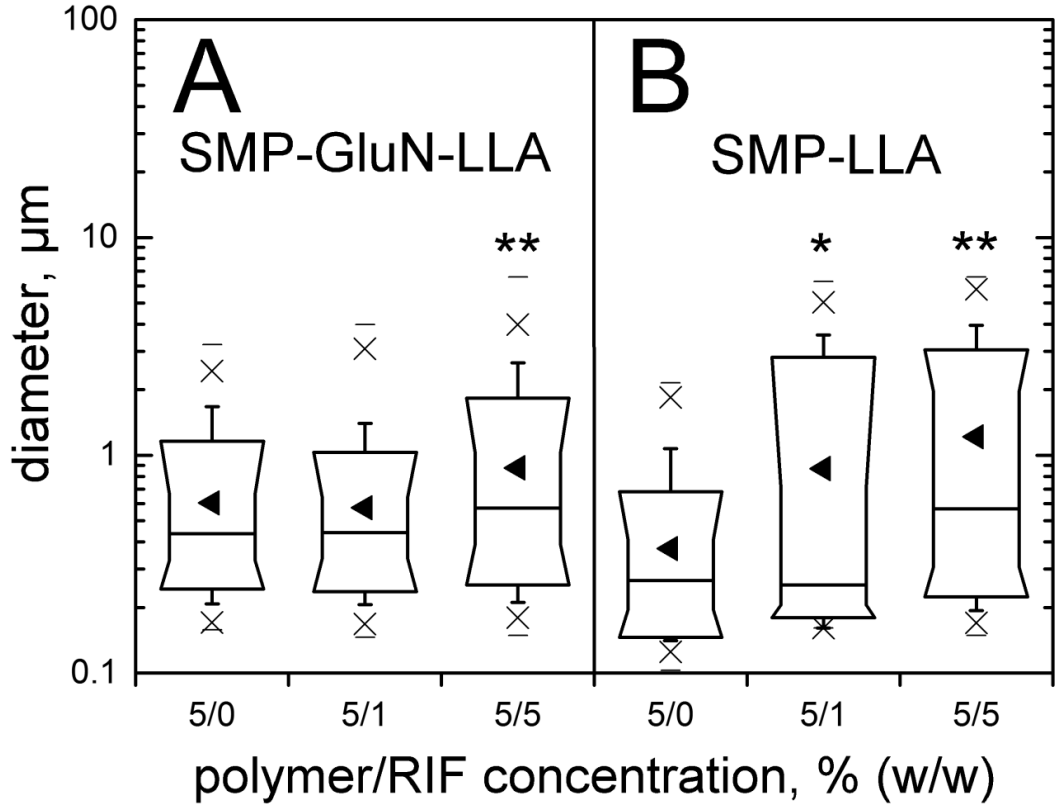

Figure 3.5. The effect of RIF loading expressed as polymer-to-RIF mass ratio, average diameter and particle size distribution. Two low molecular weight polymers were tested: A) SMP-GluN-LLA made with branched GluN-LLA, and B) SMP-LLA made with linear LMW PLA. Particles were prepared at a flow rate of 0.3 mL/h and voltage of 10 kV. There are statistically significant differences between SMP-GluN-LLA and SMP-LLA (5/5 polymer to RIF ratio) when compared with their controls, subsets A and B (**$p<0.01$). At the 5/1 ratio, only the SMP-LLA were statistically significant different when compared with its control (*$p<0.01$). Average particle size (◄), box range: 10-90%, whisker range: 5-95%, (x) 1-99%, (−) min. and max. values of particle diameter within investigated population.

3.3. Drug Entrapment Efficiency

Time-release profiles from polymeric drug-loaded nano- and microparticles are usually characterized by a set of basic stages: (1) initial burst release, (2) slow diffusion-controlled release and sometimes, a (3) phase of abrupt release caused by a final loss of structural integrity in the particles. Burst release occurs in the first few hours, and it is commonly attributed to the fraction of drug located closer to the particle surface. The objective in this experiment was to determine the amount of drug that remains after this initial release had happened. While GluN-LLA and PLA polymers are insoluble in ethanol, RIF solubility is 10 mg/mL. Thus, in order to extract the drug from the outermost layers of the particle surface, RIF-loaded particles were contacted with ethanol for 10 minutes. After ethanol treatment, particles were fully dissolved and their remaining RIF content was determined. The RIF loading efficiency measured by this ethanol leaching test indicates that the GluN-LLA polymer is superior to its linear homopolymer counterparts irrespective of molecular weight and characteristic dimensions of the particles (Table 3.2). These results correspond to the amount of RIF retained within the particles at the end of the initial 8-hour period when PBS was used. The entrapment efficiency in the microparticles is comparable to those of RIF-loaded PLGA microparticles prepared via the oil-in-water emulsification method (57-78% for PLGAs with molecular weights of 10 and 20 kDa) [40]. They are also well above those reported with RIF-loaded HMW PLA microparticles prepared via the supercritical anti-solvent method performed at comparable drug-to-polymer

ratios (40-50%) [55]. In general, the encapsulation efficiency calculated from cumulative release curves well exceeded 90% for all tested LMW systems (Table 3.2), but is extremely low for HMW PLA. This is an expected result, as the low degradation rates of this class of polymers often results in permanent drug entrapment inside polymer network [63].

Table 3.2. Encapsulation efficiency and kinetic parameters of RIF release from L-lactide based polymeric submicron and microparticles (n = 3).

Polymer	RIF: polymer ratio	Type[d]	Encapsulation efficiency, %[a]	RIF release efficiency, %[b]	Korsmeyer-Peppas equation fitting results[c]		
					n	k	R^2
GluN-LLA	1: 5	SMP-GluN-LLA	56.0±0.1	97.5	0.13	0.29	0.90
	1:10	SMP-GluN-LLA	-	96.6	0.15	0.28	0.90
LMW PLA	1: 5	SMP-LLA	15.0±0.2	98.3	0.71	0.14	0.99
GluN-LLA	1: 5	MP-GluN-LLA	71.0±1.7	93.1	0.14	0.33	0.95
	1:10	MP-GluN-LLA	-	98.1	0.22	0.25	0.93
HMW PLA	1: 5	MP-LLA	52.0±0.9	7.0	0.10	0.54	0.98

a) The drug was extracted with pure ethanol for 10 minutes and the remaining solid was analyzed via ^{1}H NMR.

b) Results based on initial (6 and 12 μM for samples with 1:10 and 1:5 RIF-to-polymer mass ratios, respectively) and cumulative drug loading.

c) $M_t/M_\infty = kt^n$, where k is the constant incorporating characteristics of the macromolecular network system and the drug , n is the exponent describing release mechanism, M_t/M_∞ is the fraction of the drug released at time t.

d) SMP: submicron particles, MP: microparticles (see Table 3.1 for details).

3.4. Rifampicin Release from Submicron- and Microparticles

The submicron- and micron-sized particles prepared with the GluN-LLA material as carrier yielded the desired results i.e., they were efficient in releasing the drug over a period of two weeks (Fig. 3.6). This efficiency was attributed to molecular interactions between RIF and the polymeric matrix. Linear polymers appeared to be less efficient than their branched counterparts in yielding strong molecular interactions with the drug. SMP-LLA prepared using a LMW PLA with a similar molecular weight to that of the glucosamine based oligomer allowed sustained drug release for 30-40 hours, as shown in Figure 3.6. However, as much as 60% of the drug was released within the first 8 hours. Similar results have been reported for PLGA (M_w = 5-15 kDa) submicron-size particles loaded with budesonide (MW= 430.5 Da) [89], and for RIF-loaded PLGA microparticles [40]. Increasing particle sizes from 165 nm to 289 nm extended the drug release time from 25-30 hours to 60 hours. Notably, submicron-particles (diameters: 169, 289 and 400 nm) prepared by these authors using a core-shell electrospray (with a coaxial, two-liquid nozzle) approach lost 60-40% of the initial drug payload in just 5 hours. This was found to take place despite the protection provided by a shell made of PLGA (100% drug encapsulation). The fact that these authors used the same drug release protocols as used in this dissertation is of utmost importance when comparing results from different sources. For example, it has been demonstrated that stirring speed significantly affects the dissolution rate profiles of RIF-loaded PDLLA microparticles [71].

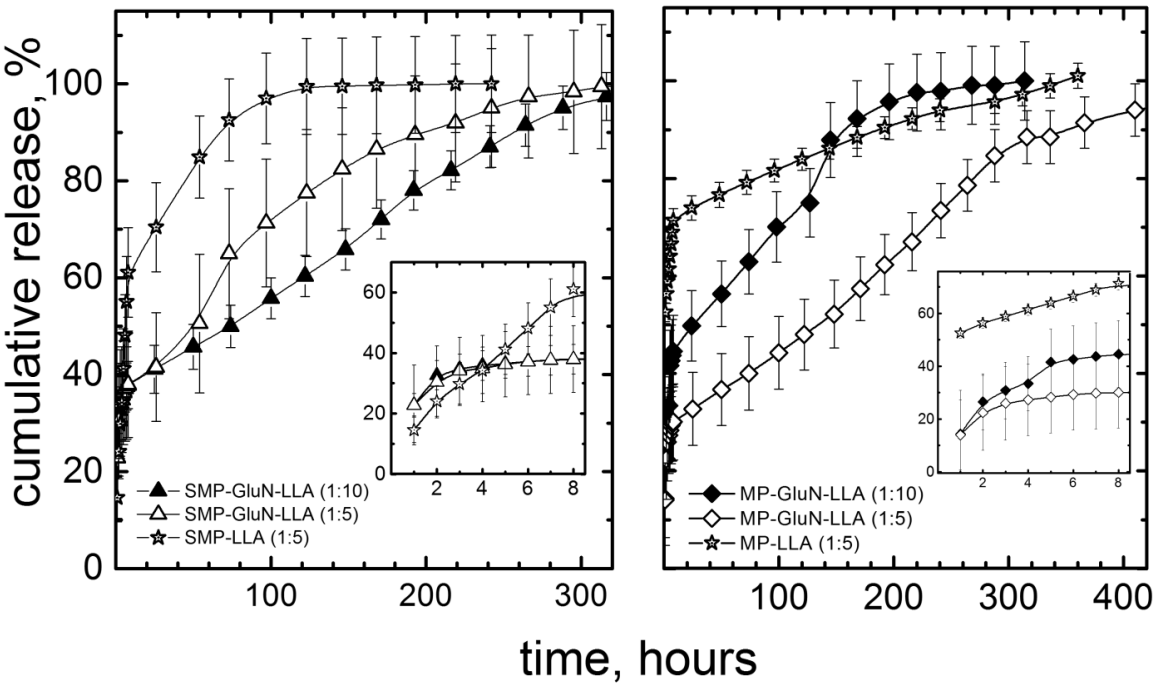

Figure 3.6. Cumulative RIF release curves from submicron and microparticles. Release curves correspond to SMP-GluN-LLA (▲), MP-GluN-LLA (♦) with RIF-to-polymer mass ratios of 1:10 and SMP-GluN-LLA (Δ), MP-GluN-LLA (◊), SMP-LLA and MP-LLA (star symbols) with RIF-to-polymer mass ratios of 1:5. Insets show the release profiles during the first 8 hours. Data represent means ± SE (n=3).

There is little difference between the drug release kinetics from nano- and microparticles made of GluN-LLA at 10 wt% and 20 wt% payloads (curves SMP-GluN-LLA (1:10) and MP-GluN-LLA(1:5) in Fig. 3.6, respectively). The ability of the new polymers to stabilize high drug payloads is also a most desirable trait, and it suggests the occurrence of a similar release mechanism for both particle diameter groups. This is consistent with particle size-encapsulation efficiency relationships reported by others [89].

For all samples, two stages of RIF release can be identified; an initial one, up to 8 hours (Scheme 3.1, Step 1 and Fig. 3.6, insets), and a delayed phase, from 8 to more than 300 hours (Scheme 3.1, Step 2 and Fig. 3.6). It is also apparent that the RIF release from SMP-LLA was mechanistically different than that from the GluN-LLA materials. This could be attributed to their different molecular architectures and functionalities, since both polymers have very similar molecular weights (Table 3.1). For LMW PLA, the drug release followed an anomalous, non-Fickian diffusion model (n = 0.71, Table 3.2) as defined by Ritger and Peppas ($0.43 < n < 0.85$) [26,29]. The Korsmeyer-Peppas equation (see annotation *c* in Table 3.2 for details) predicts a diffusion-controlled drug release mechanism for systems with diffusion exponent ‘n = 0.43’. All tested GluN-LLA submicron- and microparticulate systems have much lower n-values (0.13-0.22, Table 3.2). This is indicative of drug-polymer matrix interactions [27], and these results are also consistent with encapsulation efficiency tests and DSC results (discussed next section).

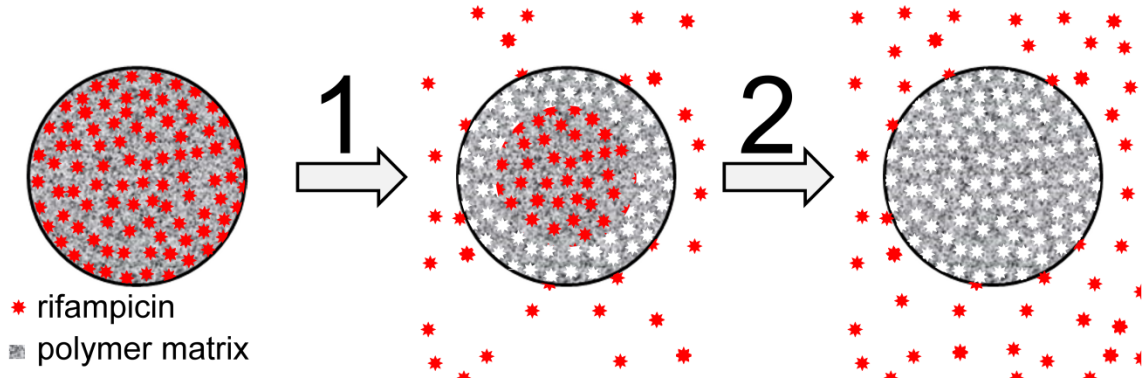

Scheme 3.1. Representation of the bimodal kinetics of RIF release from the GluN-LLA carrier: 1) initial, 2) delayed. In the delayed phase the drug passes through pores created by molecules released in the initial phase (k1 > k2). In both phases the effects of drug-polymer interactions were evident and seen as decreased values for the n exponent in the Korsmeyer-Peppas equation (Table 3.2).

3.5. Particle Degradation and Thermal Properties: Impact on Drug Release Kinetics

The degradation studies performed under identical conditions as those from drug release measurements revealed that L-lactic acid (LLA) release is proportional to the available contact surface between polymeric particles and the solution (Fig. 3.7). All tested polymers are hydroxyl-terminated and on a molecular level, the degradation mechanism for these polymers is end chain scission [90]. Both types of nanoparticles exhibited similar degradation curves, but after two weeks the LLA concentration was higher for SMP-GluN-LLA, 8.2×10^{-3} mM, than the 4.0×10^{-3} mM observed with SMP-LLA. Overall, material loss due to degradation accounts for only 5% of the initial mass in 14 days of experiment, and thus has negligible effect on the RIF release mechanism.

The DSC measurements revealed that the RIF used in this dissertation is the stable type I form (a single, sharp exothermic signal, peaking at 253°C is the only feature in its thermograms) [91]. The glass transition temperatures (T_g) for RIF-loaded submicron- and microparticles prepared with GluN-LLA increased by 8-10°C when compared to that of the pure polymer (Fig. 3.8 thermograms b, c and d) [1]. This is indicative of enhanced drug-polymer molecular interactions, i.e. RIF likely binds to terminal hydroxyl groups of GluN-LLA chains, thereby increasing its “effective molecular weight”, as evidenced by augmented T_g values. On the other hand, introduction of RIF is less likely to be responsible for the observed differences in thermal properties between pure and drug-loaded LMW PLA

nanoparticles. The as-prepared material is highly crystalline and there is no distinguishable characteristic glass transition inflection point seen in its thermogram (Fig. 3.8 f). However, rapid solvent evaporation during processing results in semi-crystalline features: T_g (46 °C) and an exothermic “cold crystallization” peak at 77°C were followed by an endothermic melting peak at 133°C. If the drug occupied exclusively the limited available amorphous polymer regions and molecular interactions were thus very weak or absent, then it would be rapidly released upon contact with the PBS solution (Fig. 3.7) or ethanol (Table 3.2).

Differences in molecular architecture have a pronounced effect on the thermal properties of these polymers: while GluN-LLA is purely amorphous, as evidenced by the previously reported DSC results, T_g = 43.7±1.3°C and the absence of the melting peak of the crystalline phase [1], the LWM PLA has semi-crystalline characteristics (Fig. 3.8 f) [92]. The DSC results suggest that chain length is a decisive crystallinity control factor for oligo-L-lactides, and transition from an amorphous to a semi-crystalline form takes place for monomer numbers higher than 10-12. In view of the results presented in this thesis, the advantages of using branched over linear molecular architectures for RIF delivery applications are apparent. The fine-tuning of the polymeric matrix crystallinity (a strategy that is sometimes used as an important drug release control factor) requires detailed knowledge of its thermal properties, and often demands the use of an additional post-processing step [93]. In matrices with reduced crystallinity, drug-polymer

interactions are enhanced. This in turn, leads to efficient dispersion of the drug within the polymer matrix, making these systems favorable for applications requiring slow release of the drug [94]. The current polymeric materials have potential for designing ultrafine particle based tuberculosis treatment systems: a typical tuberculosis treatment lasts about 6 months [4,7].

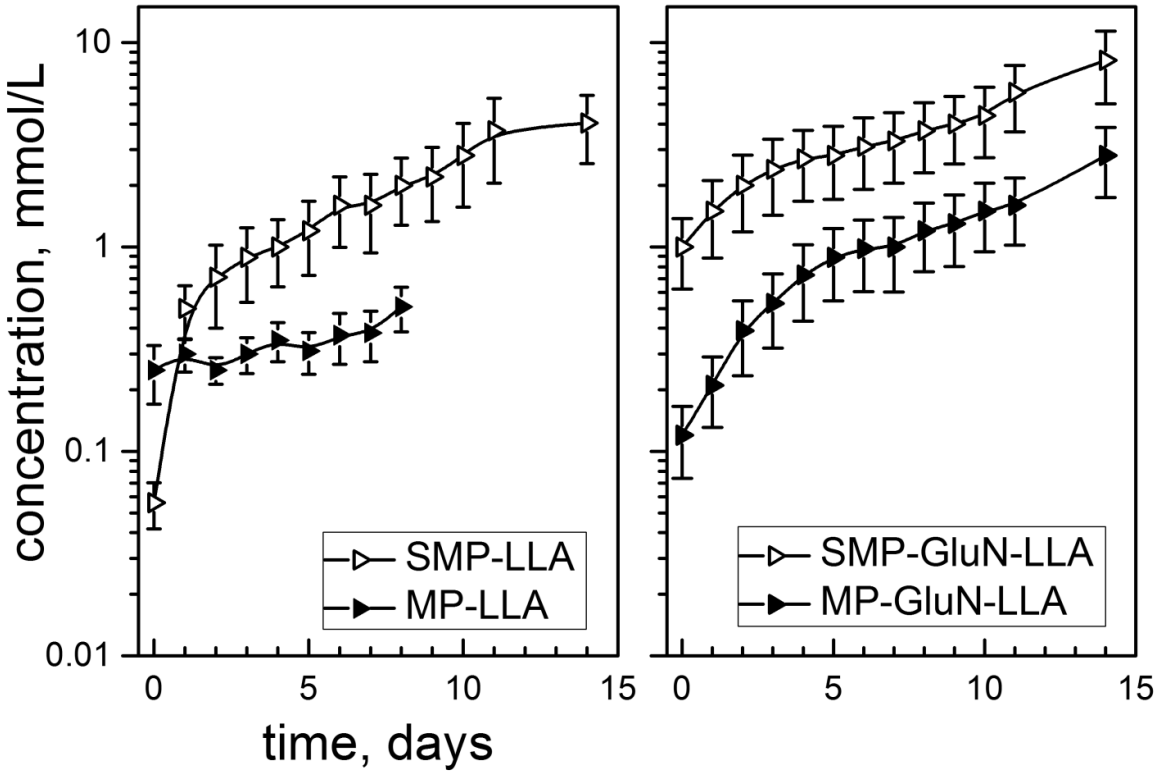

Figure 3.7. Semi-log plot of degradation of submicron- (open symbols) and micron-sized particles (filled symbols) prepared using linear (left panel) and branched (right panel) L-lactide based polymers. The release of L-lactic acid was tracked via ^{1}H NMR spectroscopy. Data represent means ± SE (n = 3).

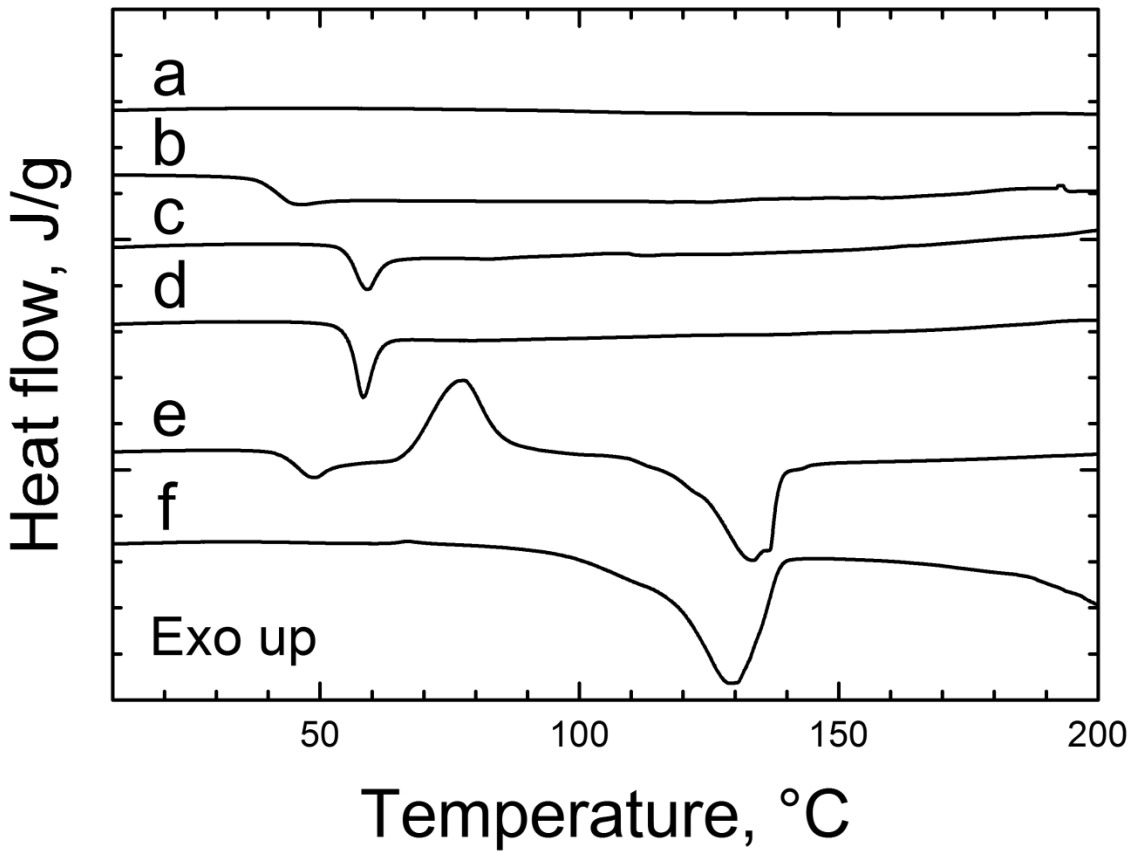

Figure 3.8. DSC thermograms. a) RIF, b) as prepared GluN-LLA polymer, c) RIF loaded SMP-GluN-LLA, d) RIF loaded MP-GluN-LLA, e) RIF loaded SMP-LLA f) as prepared LMWPLA. For samples c-e the RIF-to-polymer ratio was 1:5.

3.6. Particle Toxicity on M. Smegmatis

Chitosan, the polymeric form of glucosamine, has been regarded as a biomaterial with bactericidal properties [95,96]. Melake et al. [97] reported on its cytotoxic effect on *P. aeruginosa*, with LMW chitosan showing a higher bactericidal activity compared to its medium and high molecular weight forms. Also, Liu et al. found higher cytotoxic effects with high molecular weight chitosan. The most accepted mechanism of its antibacterial action is believed to involve the positive charge of the protonated amine groups [98].

Figure 3.9 shows the changes in % of growth area compared to control for SMP-GluN-LLA, MP-GluN-LLA, SMP-LLA and MP-LLA at 300, 600 and 1,200 μg of particles/mL. It was hypothesized a priori that the presence of a glucosamine core in GluN-LLA was going to possibly contribute some antibacterial activity on *M. smegmatis*, but as shown in Fig. 3.9, this was not the case. Changes in bactericidal activity for all particle types and for all concentrations were not statistically different when compared to the control.

However, significant statistical differences exist among particle materials (MP-GluN-LLA vs MP-LLA, # $p<0.01$). While GluN-LLA particles do not affect bacteria survival, MP-LLA seems to favor *M. smegmatis* growth. This can be explained by the high correlation between microbial adhesion and the hydrophobic/hydrophilic characteristics of the interacting surfaces. In this regard, it has been shown that the adhesion of bacteria to solid surfaces is positively affected by the surface's hydrophobicity [99,100]. *Oliveira et al.* performed adhesion experiments between

different bacteria and polymeric surfaces. These authors found surface hydrophobicity to be proportional to the number of adhering bacteria [101]. Thus, it is hypothesized that MP-LLA promotes bacterial growth compared to MP-GluN-LLA, and that bacterial adhesion to MP-LLA particles possibly facilitated bacterial proliferation.

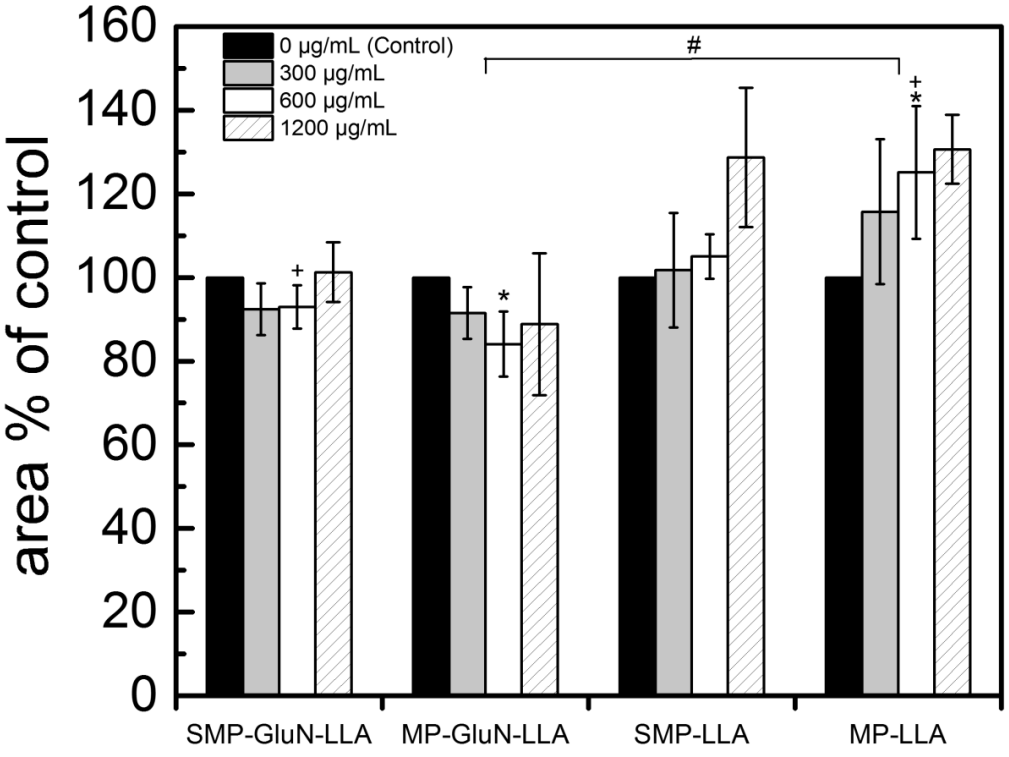

Figure 3.9. Particle toxicity on *M. smegmatis*. Mycobacteria were inoculated with different amounts of submicron- and micron-sized particles and were cultured for 24 hours. 10µL of culture was placed onto agar plates and incubated at 37ºC for three days to see visible colonies. Colony area was quantified from agar plates pictures by ImageJ software. Statistically significant differences between SMP-GluN-LLA and MP-LLA (+$p<0.05$); and between MP-GluN-LLA and MP-LLA (*$p<0.05$) at a particle concentration of 600 µg/mL, are shown. Statistically significant differences are shown between MP-LLA and MP-GluN-LLA, which is indicative of promoted bacterial growth by the linear LLA when compared to the branched GluN-LLA material (# $p<0.01$). Data represent means ± SE (n=3).

3.7. Minimum Inhibitory Concentration (MIC) and Minimum Bactericidal Concentration (MBC) of Free RIF and RIF Loaded Particles

Table 3.3 summarizes the MIC and MBC results for free and encapsulated RIF and shows pictures of bacteria after 3 days of incubation in a 7H10 agar plate. These images were used to determine the MBC values. For particles loaded at a 1:1 RIF-to-polymer mass ratio, SMP-GluN-LLA and MP-GluN-LLA showed MIC values that were about half of that of free RIF on a same dose of antibiotic basis. SMP-LLA showed MIC value 4 times lower than MIC value of RIF alone, while MP-LLA showed MIC value similar to that of RIF alone. MBC values were also affected by encapsulation: SMP-GluN-LLA and SMP-LLA showed MBC values 2 times lower than free RIF, while MBC values for MP-LLA and MP-GluN-LLA were unaffected.

Improved efficacy of antibiotics encapsulated in polymer particles and liposomes and intracellular delivery of antibiotics on different microbial strains has been reported. Mirzaee et al. [82] have found decreased values of MIC for encapsulated amikacin compared to free amikacin for *E. coli*, *P. aeruginosa*, *S. faecalis* and *S. aureus*. In the same manner, liposomes as encapsulants for amikacin, gentamicin and tobramycin reduced the MICs for highly antibiotics-resistant strains while improving the uptake of antibiotics into the bacterial cells [83]. Meropenem and tobramycin encapsulated in liposomes inhibited the growth of bacteria using sub-MIC concentrations of antibiotic [84,102]. In both cases, the bactericidal activity of the antibiotics was increased when compared with that of

the free drug. One possible explanation for this phenomenon is membrane fusion between liposomes and bacteria, which would deliver a high dose of antibiotic to the microorganism and therefore surpassing the bacteria efflux pump capacity [103,104]. Another example where the bactericidal effect was also enhanced was shown by the use of RIF-loaded particles. PLGA microparticles loaded with RIF showed a greater bactericidal effect on *Mycobacterium bovis Bacillus Calmette-Guérin* (BCG) in alveolar macrophages cells than that of RIF in solution at the same periods of time [53]. Similar results were obtained by Makino and coworkers [40], but in this case higher amounts of RIF were detected inside alveolar macrophages cells treated with RIF-loaded microparticles than when treated with RIF alone.

Antimicrobial activity of the drug-free GluN-LLA and PLA particles was evident in figure 3.9, where it is shown that the RIF-free GluN-LLA particles present no antibacterial properties on *M. smegmatis*. However, MIC reduction in RIF-loaded GluN-LLA and SMP-LLA particles indicates an increase in bacterial killing relative to free RIF. The mechanism by which RIF encapsulation on GluN-LLA particles act this way has not yet been investigated. The physicochemical characteristics of the GluN-LLA polymer are reflected by the differences in the observed MIC values. At this stage, it is possible to speculate that surface charges of the polymer attract bacteria to the particle surface exposing them to a locally high antibiotic concentration.

Table 3.3 MIC and MBC values (μg/mL) of RIF in both free, and encapsulated forms were determined by the macrobroth dilution technique. Particles were produced with a 1:1 RIF-to-polymer mass ratio. Images from agar plate of M. smegmatis incubated for 3 days after contact with RIF-loaded particles and free RIF

			RIF concentrations (μg/ml)									
	MIC	MBC	1	2	4	8	16	32	64	128	256	512
Free RIF	64	256	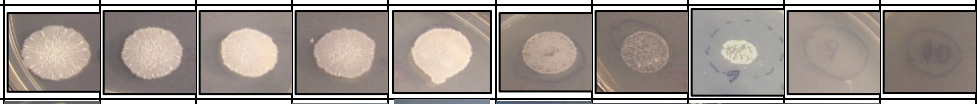									
SMP-GluN-LLA	32	128	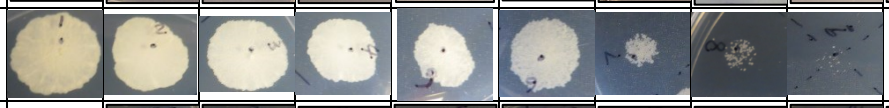									
MP-GluN-LLA	32	256	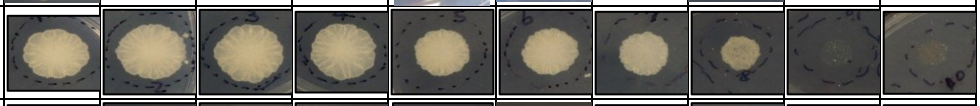									
SMP-LLA	16	128	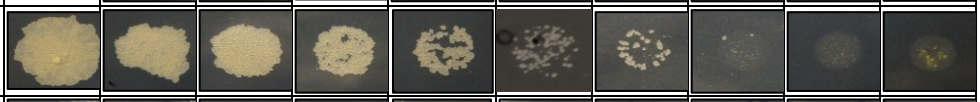									
MP-LLA	64	256	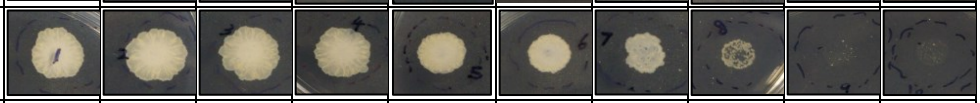									
Amount particles (μg/ml)			2	4	8	16	32	64	128	256	512	1024

3.8. Cytotoxicity of Particles on Macrophage Cells

In order to determine the cytotoxicity of the four sets of particles, the WST-8 viability assay was implemented. Figure 3.10 shows the survival rate (%) of macrophages after three days of incubation with the drug-free (no RIF) particles. Cytotoxicity was shown to be dose dependent i.e., at increasing particle doses there was an increase in cell death. Cytotoxicity was not significantly affected by the material type; at one specific dose level, all particle types showed a very similar effect. When comparing particle concentrations with the control, all particle types showed statistically significant differences at 120 and 240 μg/ml. At a concentration of 60 μg/ml, only SMP-GluN-LLA particles showed significantly different cytotoxicity levels in macrophages relative to its controls. The clear inhibition in macrophages proliferation that occurs at a particle concentration of 120 μg/ml and at higher values can be due to an accumulation of free lactic acid in the culture media. As a product of polymer degradation, lactic acid could cause a localized lethal decrease in pH. This has been previously proposed to explain the cytotoxic effect observed with LLA grafted chitosan [2]. The cytotoxicity result (~20%) of SMP-GluN-LLA particles could be also correlated with its high cellular uptake (shown in Fig. 3.11), and smaller particle size. The increasing number of particles undergoing endocytosis could cause an increment in the production of reactive oxygen species (ROS), which can lead to toxicological effects. In addition, ROS generation is strongly favored by a decrease in particle size, which necessarily translates into an increase in specific surface area [105].

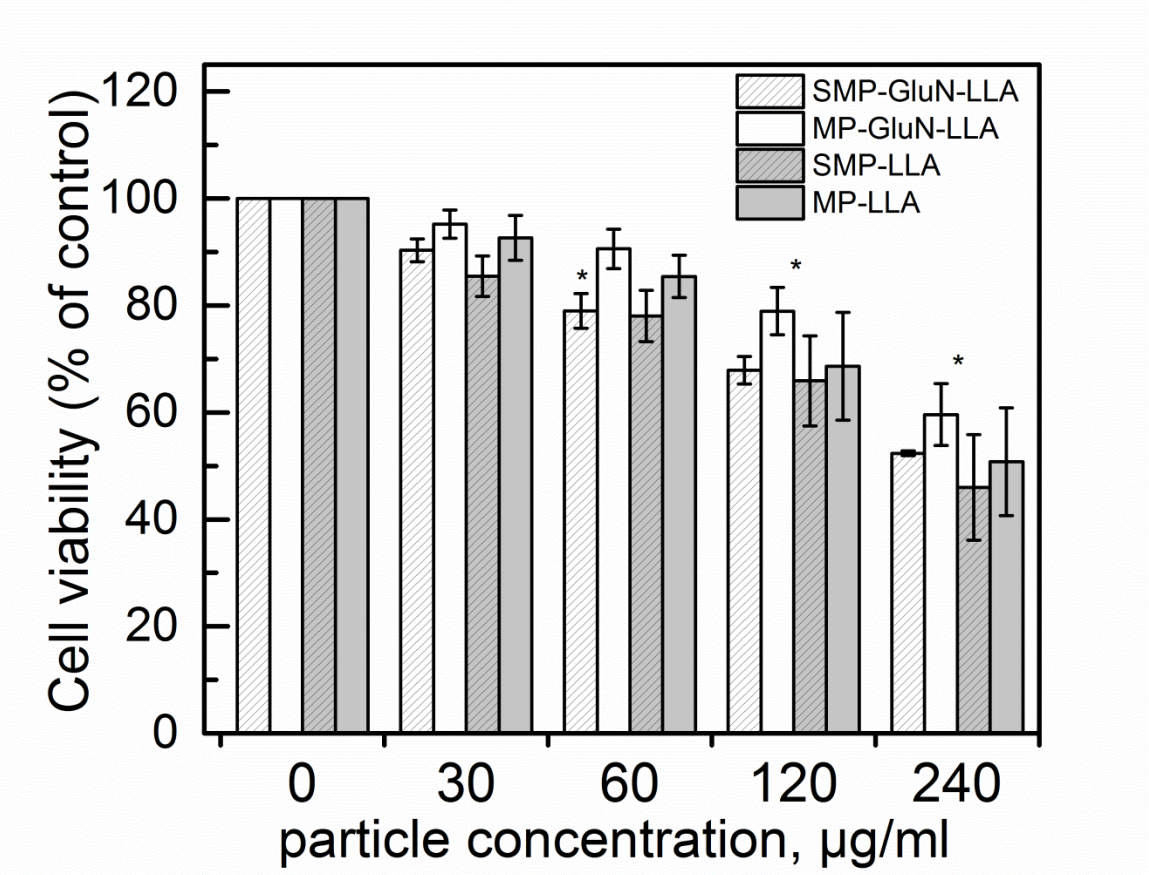

Figure 3.10. Particle cytotoxicity on J774A.1 Macrophages. Different concentrations of GluN-LLA and LLA submicron and microparticles were incubated with macrophages for 3 days. The WST-8 reagent solution was contacted with the samples for one hour prior to OD450 measurement with a BioTek Elx800 microplate reader. Cytotoxicity of submicron and microparticles increased with increasing particle doses. All particle types' cytotoxicity effects were statistically significant in terms of particle concentration when compared to their controls (*$p<0.05$). Data represent means ± SE (n=4).

3.9. Intracellular Localization of Particles by Confocal Microscopy

Particle properties such as hydrophobicity, size, shape, and surface charge affect cellular uptake [106]. When particles are introduced in the growth media they adsorb various proteins. Hydrophobic surfaces produce denaturation of adsorbed proteins, which could negatively affect the particle uptake by cells [105]. After internalization, particles can follow two major pathways leading to programmed cell death (apoptosis), namely the death receptor, or the mitochondrial pathway [107]. The polyvalent surface of nanoparticles may induce cross-linking of cellular receptors, trigger signaling processes, induce structural alterations at the cell surface, and eventually interfere with normal cell function [108,109].

Particle internalization and uptake into cells could lead to mitochondria swelling and an increase of mitochondrial membrane permeability which eventually causes mitochondrial dysfunction, ROS production, and initiation of an apoptotic signaling cascade [106]. In addition, upon internalization, particles could target lysosomes, leading to lysosomal membrane damage and dysfunction. It was reported that particle induced cell death is related to lysosomes localization in cancer cells [110]. Macrophages tend to engulf particles between 0.5-5 μm rather than nanoparticles. In addition, charged particles generally lead to better uptakes than uncharged particles [111]. In this study, GluN-LLA particles displayed higher uptake than PLA particles, as shown in Fig. 3.11.

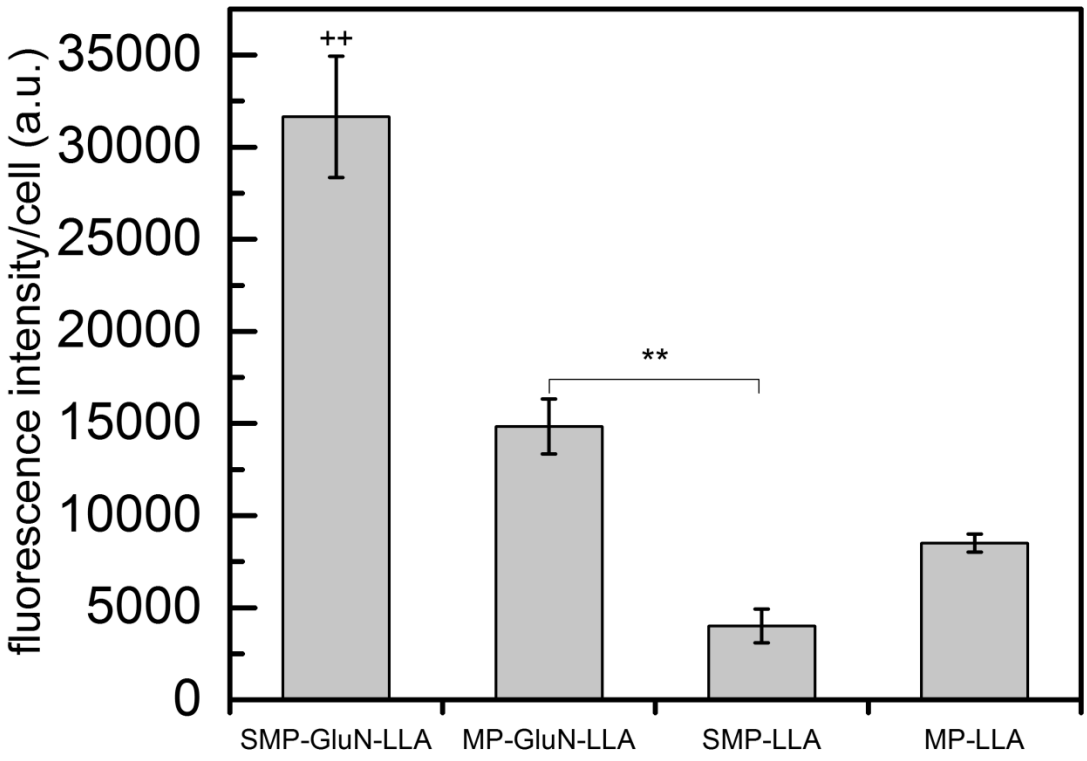

Figure 3.11. Internalization of particle by macrophages. Submicron- and micron-sized particles made out of GluN-LLA and LLA labeled with PCL-fluorescein were incubated with macrophages. Cells were washed and analyzed with confocal microscopy. The fluorescence intensity/cell of the different types of particles was quantified by ImageJ software. Macrophages showed statistically significant higher submicron- and microparticles uptake made with the branched GluN-LLA polymer than the particles made with the linear LLA polymer. Statistically significant differences (**$p<0.01$), and statistically significant differences when comparing with all populations (++$p<0.01$) are seen. Data represents means ± SE (n=4).

Previous studies showed that PLGA microparticles loaded with RIF colocalize in phago-lysosomes [112], suggesting that released RIF molecules diffuse first through the membrane of the phagosomes containing particles to the cytoplasm and then, also by diffusion, enter the phagosomes containing the bacteria. The particles studied in this thesis were internalized but surprisingly, did not colocalize in mitochondria or lysosomes. After phagocytosis, they remained in the cytoplasm (Fig. 3.12 parts A and B). What was found to be of critical relevance to the proposed medical application is that the absence of mitochondrial colocalization of particles is extremely desirable: if macrophage targeting is intended, particle colocalization in this organelle is expected to promote oxidative stresses that could lead to cell death. In these studies, particle cytotoxicity on macrophages was directly related to particle dose (Fig. 3.10). However, according to the results particle colocalization cannot be the culprit of these cytotoxic effects, as shown in Fig. 3.12 (A and B). A sustained release of RIF directly into the cytoplasm produces a strong concentration gradient within phago-lysosomes containing the bacteria. Therefore, RIF diffusion through the bacterial membrane and intracellular killing is highly improved. What is also of key relevance to the goals of this study is that GluN-LLA particles showed higher uptakes by macrophages compared to those made from LLA. This property can obviously be very desirable when considering the design of a macrophage-targeting drug delivery system [79,113]. Thus, these polymers meet two important requirements for anti-tuberculosis drug delivery applications, namely a) high macrophage uptakes and b) low cytotoxicity.

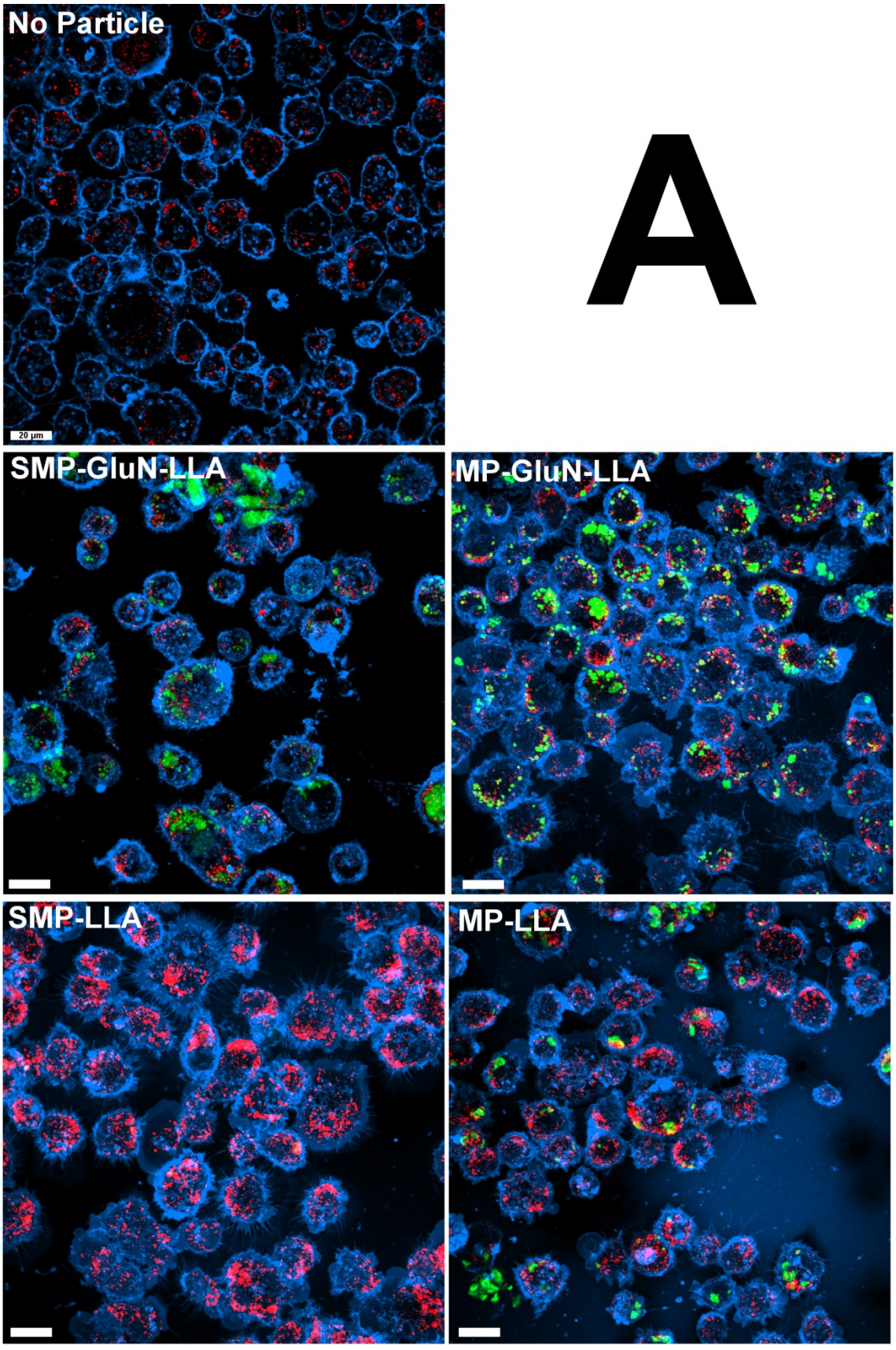
No Particle
20 µm
A
SMP-GluN-LLA
MP-GluN-LLA
SMP-LLA
MP-LLA

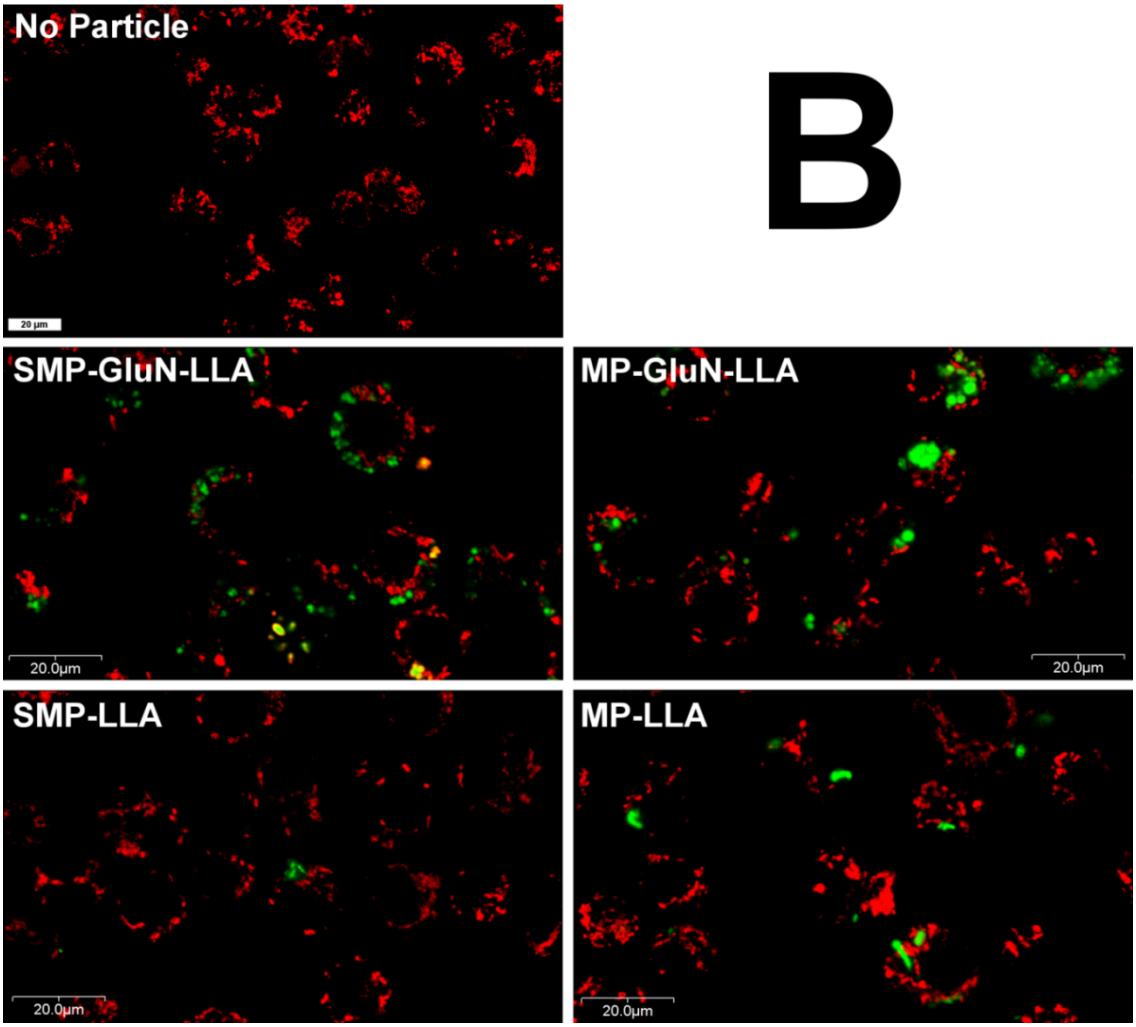

Figure 3.12. Intracellular localization of particles. Mitochondria and Lysosome were stained with mitotracker and lysotracker, respectively. In order to be visualized particles containing PCL fluorescein were produced. Part A shows the images of lysosome stained cells: cytoplasm membrane staining (blue) and lysosome staining (red) after incubation with fluorescein loaded particles (green). Part B shows the images of mitochondria stained cells: mitochondria staining (red) after incubation with fluorescein loaded particles (green). Particles are engulfed by the cells but they do not colocalize either with mitochondria or with lysosomes i.e., they stay in the cytoplasm. The scale bar is 20 µm for all images.

3.10. Intracellular Killing of M. Smegmatis

In order to evaluate the in vitro mycobactericidal effect of RIF-loaded GluN-LLA and PLA particles on M. smegmatis inside phagosomes, macrophages were first exposed to a high multiplicity of infection (MOI of 20 bacteria per cell) to facilitate infection, and after washing away the extracellular microorganism fraction, infected cells were contacted with RIF loaded particles (1:1 RIF-to-polymer mass ratio). For control and comparison purposes, free RIF and no-treatment samples were included in this experiment. To determine the intracellular killing effectiveness of free and encapsulated RIF, the ratio between the number of intracellular bacteria (c.f.u.) and the number of cells alive at the same time point was examined.

The no-treatment control experiment, which can be seen as the inset of figure 3.10, shows the cyclical behavior of killing/growth of M. smegmatis inside J774A.1 macrophages. This pattern has been observed by others [114,115]. The dynamic cycle of killing/growth phases is based on M. smegmatis' ability to grow fast, and to significantly delay phagosome maturation for a few hours. After an exponential growth stage inside the macrophages, the mycobacterium is partially or totally killed by the macrophages, depending on the extent of infection [114]. Anes et al. observed this cyclic interplay between killing and surviving of M. smegmatis in J774 macrophages cultures with MOI values of 5-10, and within 48 hours macrophages were able to kill M. smegmatis. In order to test the killing efficiency of a sustained release of RIF (from GluN-LLA particles) for a long

period of time (10 days), a very high MOI of 20 was used in this dissertation. Note that in the case of a pathogenic mycobacterium like *M. tuberculosis*, such high level of infection would naturally cause macrophage apoptosis, which in this context represents an innate defense against intracellular infection. *Lee et al*. studied macrophage apoptosis as a function of level of bacterial infection, and determined that *M. tuberculosis* rapidly induces cell apoptosis (90% in 20hrs) for MOI>10. Also, these authors' study showed that *M. smegmatis* caused a minimal effect in macrophage death at MOI 25 and 50 [116].

Since the objective of this experiment was to evaluate the performance of RIF-loaded particulate systems, and to compare with free RIF for 10 days, the amount of free or encapsulated RIF added was half of the MIC measured (see table 3.3). Considering these experimental conditions, and the induced high infection levels, total killing of bacteria was not expected. One of this thesis' goals was to determine the effect of prolonged drug release compared to free RIF. At half MIC, free RIF was very effective in killing intracellular bacteria during the first 5 days, as shown by the linear dependence found between c.f.u/cell with time (Fig. 3.13). After day 5, a cyclic pattern was apparent, indicating a reduction in RIF effectiveness. In the case of encapsulated RIF, all systems showed an oscillatory behavior, with a significant reduction in c.f.u/cell values when compared to the control. Also, contrary to free RIF, particulate systems showed to be more efficient in killing bacteria after day 5. This result could be explained by the loss of bioavailability of free RIF in culture media at 37°C, where 50% is degraded after one week [117], while the encapsulated drug may be protected

against such degradation processes. The number of intracellular bacteria per cell in GluN-LLA and PLA polymers seems to be related to the RIF release mechanism. Both GluN-LLA and SMP-LLA systems presented higher number of intracellular bacteria per cell than free RIF during the first 4 days, but superior killing efficiencies after day 6. On the other hand, the MP-PLA polymer showed a different behavior: Like with free RIF, the oscillations in this case were strongly attenuated for the first 6 days, which is probably caused by the high burst release of the drug in this system (Figure 3.6, ~50% in 1 hr and ~70% in 8hrs). From these observations, it is clear that one can use these polymers to devise a drug release system, possibly a dual particle system, whose drug release profile can be engineered virtually at will.

It is worthy of mention that after a thorough literature search, studies to assess the effect of RIF-loaded particles on *M. smegmatis* inside macrophages for more than one day were not found. To the best of the author's knowledge, this dissertation presents, for the first time, an experiment to evaluate the performance of ultrafine particles on *M. smegmatis* inside macrophages as a tuberculosis model for 10 days, and with a daily sampling frequency. The reason for the scarcity of studies dealing with this particular problem is probably due to the fact that macrophages kill *M. smegmatis* in 48 hrs for MOI values ≤ 10. For example, Sonawane et al. [118–120] have done several antibacterial assessment of starch- and chitosan-coated silver nanoparticles on infected mouse macrophages (*M.smegmatis*, MOI=10). In their work, sampling of intracellular bacteria survival was usually performed between 6 to 8 hours after infection.

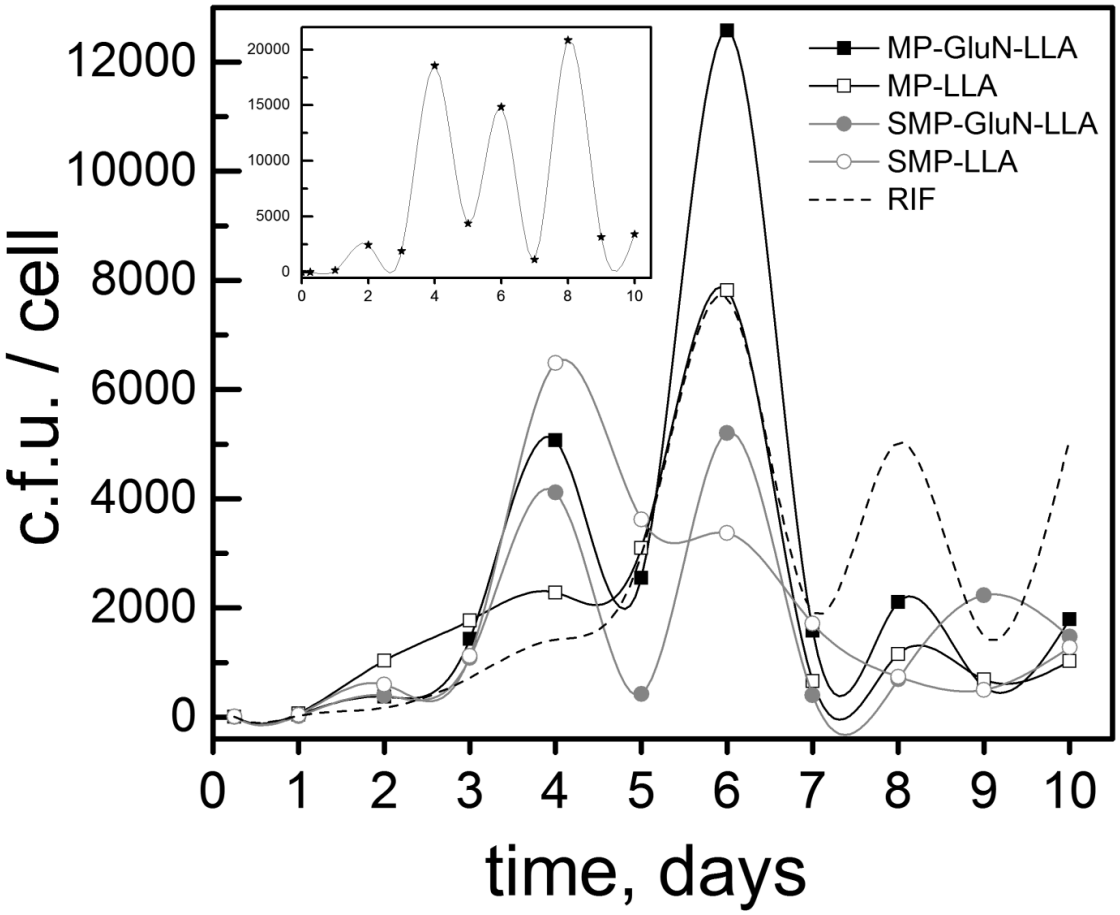

Figure 3.13. Intracellular killing of *M. smegmatis*. Macrophages were infected with *M. smegmatis* at an MOI of 1:20 (cells:bacteria). After infection macrophages were contacted with free RIF, and or RIF loaded particles. Inset shows control experiments where M. smegmatis showed a cyclic growth/killing pattern of colony forming units of intracellular M. smegmatis per macrophage cell in terms of time.

CHAPTER 4

Conclusion and Proposed Future Research

4.1. Conclusions

Using a new biocompatible polymer system based on glucosamine and L-lactide, submicron- and micron-sized particles loaded with RIF via an electrohydrodynamic atomization route were prepared. As comparator, low- and high-molecular weight poly-lactic acid materials were used. Control over particle size in a broad range was achieved by adjusting polymer concentration.

A sustained RIF release from submicron- and micro-sized particles for 14 days *in vitro* was observed. These temporal profiles are composed of two clearly discernible stages: an initial drug release phase (up to 8 hours) from the outermost layers of the particles, followed by a delayed release phase. A nearly linear RIF release profile was observed for several days in the delayed phase for GluN-LLA submicron- and microparticles, and for the drug loadings of 10 and 20%, respectively. After 14 days, degradation of the polymer matrix accounts for a loss of only 5% of the initial particulate mass, and its effect on the drug release mechanism is likely negligible. The Korsmeyer-Peppas equation represented the observed drug release behavior very well, which indicated that a modified diffusion-controlled release kinetics mechanism of RIF took place in all tested GluN-LLA systems. Low diffusion exponent values are indicative of enhanced drug-polymer matrix interactions. This is consistent with DSC results, i.e. a shift of 8-10°C towards higher temperatures in the observed glass transition temperature for drug loaded GluN-LLA particles. Drug encapsulation efficiency evaluated via ethanol leaching is also in line with the DSC findings. Four terminal

hydroxyl and one primary amine groups are present in GluN-LLA molecules, as opposed to just a single terminal hydroxyl moiety in the linear LMW PLA. Increased hydroxyl density could facilitate the enhancement of polymer-RIF interactions (five hydroxyl groups in the drug molecule) via hydrogen bonding. Thus, molecular affinity seemed to have been the dominant release mechanism in this case.

Polymers that show high macrophage internalization without colocalization into different organelles are excellent candidates for the production of anti-tuberculosis drug carrier particles. This was the case with glucosamine/L-lactide based polymers: the drug-loaded particles remain in the cytoplasm, releasing RIF in close proximity to intracellular bacteria. Intracellular killing of *M. smegmatis* by different particles showed a cyclic interplay between live and dead bacteria. The presence of free or encapsulated RIF at sub-MIC concentrations was effective in reducing the number of bacteria per cell compared to the control. It is suggested that the combination of different particle types and sizes involving at least one type of particle made from the new polymers used in this study will ultimately lead to the design of a system with optimal drug release profiles.

This thesis' overarching goal was to design a drug delivery system capable of attacking the microorganism over a long period of time and with just one dose. For a given set of chemical characteristics that could lead to carrier-drug interactions, polymeric materials with higher branching point densities and with amorphous structures may in principle extend RIF release times. The

development of such materials is an important area of research in the field of design of drug delivery systems for the treatment of tuberculosis. The *in vitro* results presented in this dissertation indicate that glucosamine/L-lactide polymeric systems are promising candidates for this particular application.

4.2 - Proposed Future Work

This dissertation has presented an approach for the development of a sustained drug delivery system as a potentially viable model for the treatment of tuberculosis. The proposed system is composed of biodegradable rifampicin (RIF)-loaded ultrafine particles. However, there would be certain areas to explore before the proposed drug delivery system can be developed into an effective nasal delivery vehicle for tuberculosis. This section will describe possible future directions in the evaluation of GluN-LLA ultrafine particles for RIF lung delivery.

(1) In vitro evaluation of a Dual-Particle System. Section 3.10 in Chapter 3 discusses the *in vitro* intracellular killing of the model bacteria from free and encapsulated RIF, and the superior performance of the particle system was demonstrated. In addition, and especially after Figure 3.13 is reexamined, one future experiment can be envisioned, namely the *in vitro* evaluation of a dual particle system for the RIF lung delivery as a treatment for tuberculosis. Specifically, a system containing MP-GluN-LLA and SMP-LLA would potentially combine the individual qualities of each particulate system. MP-LLA burst release would provide high extracellular RIF concentrations during the first eight hours of

the treatment (figure 3.6), and keep releasing the remaining drug in it over the course of 3-4 days. On the other hand, SMP-GluN-LLA (which undergoes endocytosis) would provide an intracellular sustained release of the drug for more than 12 days. Since drug release profiles of dual-particle systems can in principle be engineered at will, superior bacterial killing by such approach can be envisioned. *In vitro* drug release studies and intracellular killing evaluation using the procedures explained in sections 2.2.3 and 2.5.4 could then be proposed for the dual-particle systems listed in table 4.1. If one or two such systems showed improved behavior *in vitro* over the already tested single particle system, they would offer the possibility for advancing to an optimization stage, and ultimately toward *in vivo* research phase.

Table 4.1. Dual particle systems (PDS) proposed for future experimentation

PDS	Particle combinations in a 1:1 ratio (initially)
PDS-1	SMP-GluN-LLA and SMP-LLA
PDS-2	MP-GluN-LLA and SMP-LLA
PDS-3	MP-GluN-LLA and MP-LLA
PDS-4	SMP-GluN-LLA and MP-LLA

For work beyond this dissertation, *in vivo* experimentation would be the next logical step to evaluate GluN-LLA nano- and microparticles for their intended purpose. To put things in perspective, *in vivo* studies have only demonstrated thus far sustained release of RIF from PLGA nanoparticles for up to 4 days (but via single oral administration [121]), so the need for improving these particle formulations for delayed release of RIF remains strong, and the need for investigating other forms of drug delivery (e.g., intranasal) remains unaddressed.

The development of new polymeric material variants within this drug carrier family, for example with a higher degree of branching and amorphous structures that enhance RIF-matrix interactions, could in principle lead to additional improvements. In summary, the *in vitro* performance of GluN-LLA particles showed the essential features of high drug loading, slow sustained release, endocytosis by macrophages, MIC reduction, and intracellular killing of bacteria. These characteristics would warrant *in vivo* experimentation, even if these systems were by sheer luck, close to the optimum formulation. Such experiments are proposed below.

(2) Intracellular killing assessment of M. tuberculosis in a mouse model.
Animal handling and experimentation should be conducted following IACUC approval, standard protocols and approved guidelines. A mouse model is convenient and economical, yet with an animal size large enough to allow for drug administration, blood sampling and various tissue analyses and pharmokinetics [122–125]. For this study, Swiss mice would be infected with *M.*

tuberculosis H37Rv bacilli through the conventional aerosol route (Glascol inhalation route) [122–124], and randomly divided into an ideal set of groups as described in table 4.2. For statistic validation, each group would be composed of at least four animals, but ideally six. For comparison purposes, mice in control group 1 would not be treated with RIF, and groups 2-to-4 would receive “bank” particles (no drug) via the inhalation route. Animals in groups 5 to 13 would be treated weekly by inhalation of RIF-loaded particles at three doses levels (see Table 4.2). Group 14 would be composed by mice receiving free RIF orally seven days at a week. As it was mentioned before, a combination of GluN-LLA and PLA particles for the lung delivery of RIF is a priori promising, and for this reason, groups 4, 10 and 13 are optional, depending on their performance in *in vitro* experiments. Twenty one days after infection [123], each group would be treated as indicated in table 4.2.

Table 4.2. Proposed Swiss mice groups for *in vivo* experimentation for oral and inhalation treatments.

Group	Treatment would start 21 days post infection	Treatment and dosage
1	Untreated control	No treatment
2	SMP-GluN-LLA (weekly dose)	Inhalation Treatment with drug-free particles No RIF dose
3	MP-GluN-LLA (weekly dose)	
4*	PDS-X (weekly dose)	
5	RIF loaded SMP-GluN-LLA (weekly dose 1)	Inhalation Treatment with RIF-loaded particles Dose 1 = O x 7 = W
6	RIF loaded MP-GluN-LLA (weekly dose 1)	
7*	RIF loaded PDS-X (weekly dose 1)	
8	RIF loaded SMP-GluN-LLA (weekly dose 2)	Inhalation Treatment with RIF-loaded particles Dose 2 = W/2
9	RIF loaded MP-GluN-LLA (weekly dose 2)	
10*	RIF loaded PDS-X (weekly dose 2)	
11	RIF loaded SMP-GluN-LLA (weekly dose 3)	Inhalation Treatment with RIF-loaded particles Dose 2 = W/4
12	RIF loaded MP-GluN-LLA (weekly dose 3)	
13*	RIF loaded PDS-X (weekly dose 3)	
14	RIF (daily dose O)	Oral treatment with free RIF dose (O) would be administered daily per week W=O x 7
*optional groups depending on previous dual particle systems *in vitro* experimentation		

In order to demonstrate improvement over conventional oral treatment against tuberculosis in terms of patient compliance and drug side effects reduction, the weekly inhalation doses of RIF loaded GluN-LLA particles for groups 8-to-10 and 11-to-13 would represent ½ and ¼ respectively of the weekly total free RIF orally administrated to group 14. Groups 5 to 7 would receive same amount of RIF than group 14 in a week. Thus, group 14 would receive an oral *daily dose* of 10 mg/kg of animal of RIF [122] for the entire course of the experiment (two weeks). Mice on groups 2 to 4, 5 to 7, 8 to 10 and 11 to 13 would be placed in a nose-only inhalation chamber (ADG Developments, Ltd, Herts, UK) to receive a *weekly RIF dose* loaded particles of 0, 70, 35 and 17.5 mg/kg of animal, respectively. SMP-GLUN-LLA and MP-GluN-LLA particles with 1:1 RIF-to-polymer mass ratio would be employed for this experiment. One day after the completion of the two-week treatment, mice from all groups would be euthanized. Then, lungs and spleen would be harvested, homogenized and placed in appropriate cell culture medium for *M. tuberculosis* loads determination, as explained elsewhere [123,124,126].

Results from this experiment would provide first-hand insight into the *in vivo* effectiveness of these particulate systems, and eventually point toward preclinical and clinical product development phases. Note that reductions of the recovered bacterial c.f.u. would be expected for all groups administrated with orally or inhaled RIF, when compared with the no administration of the drug (control groups 1 to 4). Likewise, any significant reduction, or even similar counting pf bacteria loads in groups 5 to 13 (inhalation treatment) as compared with group 14 (oral treatment) would be taken as a positive result. As described in table 4.2,

when compared with oral treatment, RIF loaded particles used via the inhalation route should improve dosing regimen (less frequency) and groups 8-to-13 decrease the amount of drug delivered to mice. These effects would lead to a decrease in side effects and improve compliance of the patients.

Others *in vivo* experiments would be of interest, such as the ***(3) assessment of drug concentration in alveolar macrophages, and serum*** after administration of the 'nose-only' and oral RIF loaded particles [124,126]; and ***(4) phagocytosis activity by generation of nitric oxide (NO)***. These two tests are typically performed by analyzing the bronchioalveolar lavage (BAL) fluid that can be collected at several intervals after mice are dosed (only first dose in the treatment explained above). *Parikh et al.* [126]collected BAL from animals at intervals of 15, 30, 60, 90, 120, 150, 180, and 240 minutes, which produced important information about drug uptake and phagocytic stimulation. The procedures to determine drug concentration in macrophages and NO from BAL fluid are available elsewhere [124,126].

As previously mentioned, the main advantage of lung delivery through inhalation therapy is the potential reduction of drug side effects, which is achieved by decreasing the amount of RIF delivered over the treatment period. This is possible as a result of avoiding first-pass metabolism and reducing renal clearance [127]. An adverse effect of RIF and the other first-line anti-tuberculosis drugs such as isoniazid, pyrazinamide and ethambutol often affects compliance of the patient [13]. The most serious side effect of RIF is hepatotoxicity, and it

should be the focus of any future *in vivo* toxicity studies our group may eventually desire to pursue. RIF toxicity can be assessed by a ***(5) study of liver functions*** such as serum glutamic oxaloacetic transaminase (SGOT) and serum glutamic pyruvic transaminase (SGPT) [13,126]. Elevated levels of these enzymes in serum samples collected from mice groups would serve as indicative of liver damage. Other valuable set of toxicity tests would be the ***(6) histological examination*** of some organs after treatment, such as lung and liver. In brief, these tissues would have to be subjected to H&R staining, and then analyzed via high resolution microscopy [126].

The ability to control side chain lengths (SCL) of the LLA building block in the GluN-LLA copolymer has been suggested in this dissertation as an important feature for tuning hydrophobic-hydrophilic characteristics of the particles. Table 4.3 shows four GluN-LLA copolymers with different SCLs that have been synthesized in the past [1]. Since only GluN-LLA 1:32 has been investigated in this dissertation with excellent results, the possibility of future experimentation with formulation naturally arises. The working hypothesis would be that different SCL should lead to modified RIF-matrix interactions, and as a consequence to different drug release profiles. As starting point, ultrafine GluN-LLA RIF loading particles would be prepared using GluN-LLA 1:16, 1:24 and 1:40, and ***(7) in vitro drug release determination of new GluN-LLA particulate system*** would be performed. Results from this experiment would confirm the conclusions presented in this dissertation with regard to the mechanism of drug-matrix interaction, or provide new valuable information.

Table 4.3. Different molar ratios of LLA grafted glucosamine (GluN-LLA)

GluN-LLA type	Average Molecular Weight, Mn (H NMR)	SCL
1:16	1800	6.3
1:24	2000	8.7
1:32	3100	10.8
1:40	3700	12.2

This dissertation has shown the possibility of producing an ultrafine GluN-LLA particle system as encapsulant for sustained release of RIF for more than 14 days. These biodegradable particles showed biocompatibility and high endocytosis by macrophages, which are crucial characteristics for proposing new approaches to treat tuberculosis. However, the subject system proposes the intracellular killing of M. tuberculosis using RIF alone. In the conventional 6-month treatment of tuberculosis, multidrug therapy is necessary to not only cure patients, but also to prevent the appearance of drug resistance strains. The World Health Organization (WHO) strongly recommends the use of multidrug treatments since monotherapy (use of a single drug) is one of the causes of the MDR-tuberculosis spreading [9]. For this reason, it is reasonable to propose as future work the following: ***(7) encapsulation of Ethambutol, Isoniazid and Streptomycin*** and (***8) in vitro evaluation of multidrug systems on M. smegmatis.*** As it can be seen in Figure 4.1, streptomycin possesses an important number of –OH groups that could produce the hydrogen interaction needed to yield a strong drug-GluN-LLA interaction, with a concomitant slowing of the drug release kinetics for this particulate system.

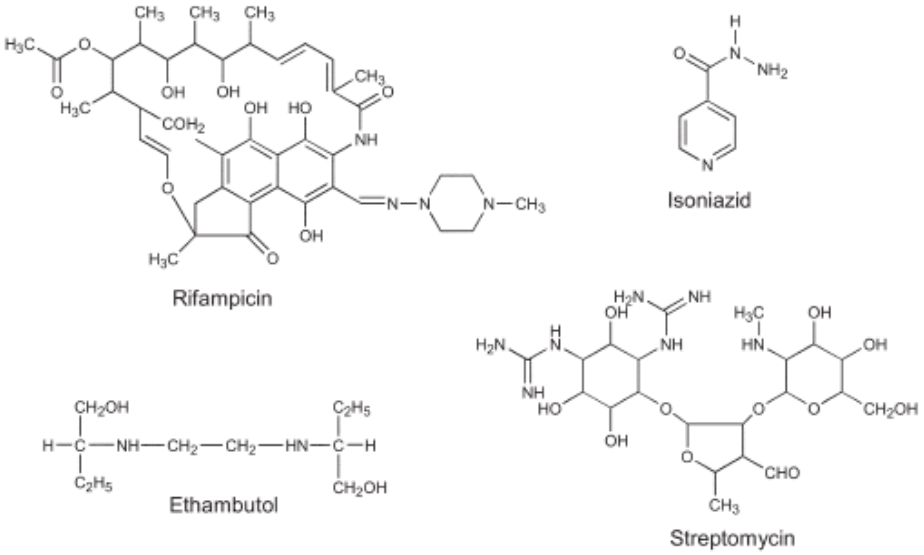

Figure 4.1. First line anti-tuberculosis drugs

References

1. Skotak M, Larsen G. Visible light-absorbing biocompatible polymers based on L-lactide and aminosugars: preparation and characterization. Polym Int. John Wiley & Sons, Ltd.; 2010 Oct;59:1331–1338. .
2. Skotak M, Leonov AP, Larsen G, Noriega S, Subramanian A. Biocompatible and biodegradable ultrafine fibrillar scaffold materials for tissue engineering by facile grafting of L-lactide onto chitosan. Biomacromolecules. 2008;9:1902–1908. .
3. Reyrat J-M, Kahn D. Mycobacterium smegmatis: an absurd model for tuberculosis? Trends Microbiol. 2001 Oct;9:472–473. .
4. WHO. Global Tuberculosis Report 2014. World Heal Organ. 2014. p. 306. .
5. Welin A, Lerm M. Inside or outside the phagosome? the controversy of the intracellular localization of Mycobacterium tuberculosis. Tuberculosis. 2012. p. 113–120. .
6. Ranjita S, Loaye AS, Khalil M. Present status of nanoparticle research for treatment of tuberculosis. J Pharm Pharm Sci. 2011;14:100–116. .
7. Du Toit LC, Pillay V, Danckwerts MP. Tuberculosis chemotherapy: current drug delivery approaches. Respir Res. BioMed Central; 2006;7:118. .
8. Gengenbacher M, Kaufmann SHE. Mycobacterium tuberculosis : success through dormancy. FEMS Microbiol Rev. 2012;36:514–532. .
9. Zhang Y, Yew WW. Mechanisms of drug resistance in Mycobacterium tuberculosis. Int J Tuberc lung Dis. 2009;13:1320–1330. .

10. Cohen T, Sommers B, Murray M. The effect of drug resistance on the fitness of Mycobacterium tuberculosis. Lancet Infect Dis. 2003 Jan;3:13–21. .

11. Wehrli W. Rifampin: mechanisms of action and resistance. Rev Infect Dis. 1983;5 Suppl 3:S407–S411. .

12. Suarez S, O'Hara P, Kazantseva M, Newcomer CE, Hopfer R, McMurray DN, Hickey AJ. Airways delivery of rifampicin microparticles for the treatment of tuberculosis. J Antimicrob Chemother. 2001;48:431–434. .

13. Tostmann A, Boeree MJ, Aarnoutse RE, De Lange WCM, Van Der Ven AJAM, Dekhuijzen R. Antituberculosis drug-induced hepatotoxicity: Concise up-to-date review. J Gastroenterol Hepatol. 2008. p. 192–202. .

14. Zumla A, Nahid P, Cole ST. Advances in the development of new tuberculosis drugs and treatment regimens. Nat Rev Drug Discov. 2013;12:388–404. .

15. Vyas S., Kannan M., Jain S, Mishra V, Singh P. Design of liposomal aerosols for improved delivery of rifampicin to alveolar macrophages. Int J Pharm. 2004 Jan;269:37–49. .

16. Fenaroli F, Westmoreland D, Benjaminsen J, Kolstad T, Skjeldal FM, Meijer A, van der Vaart M, Ulanova L, Roos N, Nyström B, Hildahl J, Griffiths G. Nanoparticles as Drug Delivery System against Tuberculosis in Zebrafish Embryos: Direct Visualisation and Treatment. ACS Nano. 2014; .

17. Vilar G, Tulla-Puche J, Albericio F. Polymers and drug delivery systems. Curr Drug Deliv. 2012;9:367–394. .

18. Kim KK, Pack DW. Microspheres for Drug Delivery. Biol Biomed Nanotechnol. 2006;19–50. .

19. Fu Y, Kao WJ. Drug release kinetics and transport mechanisms of non-degradable and degradable polymeric delivery systems. Expert Opin Drug Deliv. 2010;7:429–444. .

20. Ratner BD, Hoffman AS, Schoen FJ, Lemons JE. biomaterials science: An Introduction to Materials in Medicine. Chem Eng. 2004. .

21. Coupe AJ, Davis SS, Wilding IR. Variation in gastrointestinal transit of pharmaceutical dosage forms in healthy subjects. Pharm Res. 1991;8:360–364. .

22. Shishoo CJ, Shah SA, Rathod IS, Savale SS, Vora MJ. Impaired bioavailability of rifampicin in presence of isoniazid from fixed dose combination (FDC) formulation. Int J Pharm. 2001;228:53–67. .

23. Mahapatro A, Singh DK. Biodegradable nanoparticles are excellent vehicle for site directed in-vivo delivery of drugs and vaccines. J Nanobiotechnology. 2011. p. 55. .

24. Murnane D, Hutter V, Harang M. Pharmaceutical Aerosols and Pulmonary Drug Delivery. Aerosol Sci Technol Appl. 2014. p. 221–269. .

25. Siepmann J, Siepmann F. Mathematical modeling of drug delivery. Int J Pharm. 2008. p. 328–343. .

26. Ritger PL, Peppas NA. A simple equation for description of solute release I. Fickian and non-fickian release from non-swellable devices in the form of

slabs, spheres, cylinders or discs. J Control Release. Elsevier; 1987;5:23–36. .

27. Yu H, Jia Y, Yao C, Lu Y. PCL/PEG core/sheath fibers with controlled drug release rate fabricated on the basis of a novel combined technique. Int J Pharm. 2014;469:17–22. .

28. Lao LL, Venkatraman SS, Peppas NA. Modeling of drug release from biodegradable polymer blends. Eur J Pharm Biopharm. 2008;70:796–803. .

29. Ritger PL, Peppas NA. A simple equation for description of solute release II. Fickian and anomalous release from swellable devices. J Control Release. 1987. p. 37–42. .

30. Peppas NA, Sahlin JJ. A simple equation for the description of solute release. III. Coupling of diffusion and relaxation. Int J Pharm. 1989;57:169–172. .

31. Rajan M, Raj V. ENCAPSULATION, CHARACTERISATION AND IN-VITRO RELEASE OF ANTI-TUBERCULOSIS DRUG USING CHITOSAN – POLY ETHYLENE GLYCOL NANOPARTICLES. Int J Pharm Pharm Sci. 2012;4:255–259. .

32. Ahmad Z, Sharma S, Khuller GK. Chemotherapeutic evaluation of alginate nanoparticle-encapsulated azole antifungal and antitubercular drugs against murine tuberculosis. Nanomedicine Nanotechnol Biol Med. 2007;3:239–243. .

33. Choonara YE, Pillay V, Ndesendo VMK, du Toit LC, Kumar P, Khan RA, Murphy CS, Jarvis D-L. Polymeric emulsion and crosslink-mediated

synthesis of super-stable nanoparticles as sustained-release anti-tuberculosis drug carriers. Colloids Surfaces B Biointerfaces. 2011 Oct;87:243–254. .

34. Manca ML, Cassano R, Valenti D, Trombino S, Ferrarelli T, Picci N, Fadda AM, Manconi M. Isoniazid-gelatin conjugate microparticles containing rifampicin for the treatment of tuberculosis. J Pharm Pharmacol. 2013;65:1302–1311. .
35. Grobler AF. CHAPTER 5 : THE POTENTIAL OF PHEROID ™ TECHNOLOGY IN THE TREATMENT OF INFECTIOUS. p. 177–260. .
36. Doan TVP, Olivier JC. Preparation of rifampicin-loaded PLGA microspheres for lung delivery as aerosol by premix membrane homogenization. Int J Pharm. Elsevier B.V.; 2009;382:61–66. .
37. Doan TVP, Couet W, Olivier JC. Formulation and in vitro characterization of inhalable rifampicin-loaded PLGA microspheres for sustained lung delivery. Int J Pharm. 2011 Jul;414:112–117. .
38. Hong Y, Li Y, Yin Y, Li D, Zou G. Electrohydrodynamic atomization of quasi-monodisperse drug-loaded spherical/wrinkled microparticles. J Aerosol Sci. 2008 Jun;39:525–536. .
39. Ito F, Makino K. Preparation and properties of monodispersed rifampicin-loaded poly(lactide-co-glycolide) microspheres. Colloids surfaces B Biointerfaces. 2004;39:17–21. .
40. Makino K, Nakajima T, Shikamura M, Ito F, Ando S, Kochi C, Inagawa H, Soma G-I, Terada H. Efficient intracellular delivery of rifampicin to alveolar

macrophages using rifampicin-loaded PLGA microspheres: effects of molecular weight and composition of PLGA on release of rifampicin. Colloids surfaces B Biointerfaces. 2004;36:35–42. .

41. Tomoda K, Kojima S, Kajimoto M, Watanabe D, Nakajima T, Makino K. Effects of pulmonary surfactant system on rifampicin release from rifampicin-loaded PLGA microspheres. Colloids surfaces B Biointerfaces. 2005;45:1–6. .

42. Yoshida A, Matumoto M, Hshizume H, Oba Y, Tomishige T, Inagawa H, Kohchi C, Hino M, Ito F, Tomoda K, Nakajima T, Makino K, Terada H, Hori H, Soma G-I. Selective delivery of rifampicin incorporated into poly(DL-lactic-co-glycolic) acid microspheres after phagocytotic uptake by alveolar macrophages, and the killing effect against intracellular Mycobacterium bovis Calmette-Guérin. Microbes Infect Inst Pasteur. 2006;8:2484–2491. .

43. Makadia HK, Siegel SJ. Poly Lactic-co-Glycolic Acid (PLGA) as Biodegradable Controlled Drug Delivery Carrier. Polymers (Basel). 2011;3:1377–1397. .

44. Dutt M, Khuller GK. Chemotherapy of Mycobacterium tuberculosis infections in mice with a combination of isoniazid and rifampicin entrapped in Poly (DL-lactide-co-glycolide) microparticles. J Antimicrob Chemother. 2001;47:829–835. .

45. Ain Q, Sharma S, Garg SK, Khuller GK. Role of poly [DL-lactide-co-glycolide] in development of a sustained oral delivery system for antitubercular drug(s). Int J Pharm. 2002;239:37–46. .

46. Sharma A, Pandey R, Sharma S, Khuller GK. Chemotherapeutic efficacy of poly (DL-lactide-co-glycolide) nanoparticle encapsulated antitubercular drugs at sub-therapeutic dose against experimental tuberculosis. Int J Antimicrob Agents. 2004;24:599–604. .

47. Pandey R, Sharma A, Zahoor a, Sharma S, Khuller GK, Prasad B. Poly (DL-lactide-co-glycolide) nanoparticle-based inhalable sustained drug delivery system for experimental tuberculosis. J Antimicrob Chemother. 2003 Dec;52:981–986. .

48. Pond S, Tozer T. First-Pass Elimination Basic Concepts and Clinical Consequences. Clin Pharmacokinet. Springer International Publishing; 1984;9:1–25. .

49. Mortensen NP, Durham P, Hickey AJ. The role of particle physico-chemical properties in pulmonary drug delivery for tuberculosis therapy. J Microencapsul. Informa Healthcare; 2014 Aug;31:785–795. .

50. Hanif SNM, Garcia-Contreras L. Pharmaceutical aerosols for the treatment and prevention of Tuberculosis. Front Cell Infect Microbiol. 2012. .

51. Sharma R, Saxena D, Dwivedi AK, Misra A. Inhalable microparticles containing drug combinations to target alveolar macrophages for treatment of pulmonary tuberculosis. Pharm Res. 2001;18:1405–1410. .

52. O'Hara P, Hickey AJ. Respirable PLGA microspheres containing rifampicin for the treatment of tuberculosis: Manufacture and characterization. Pharm Res. 2000;17:955–961. .

53. Hirota K, Hasegawa T, Nakajima T, Inagawa H, Kohchi C, Soma G-I, Makino K, Terada H. Delivery of rifampicin-PLGA microspheres into alveolar macrophages is promising for treatment of tuberculosis. J Control Release. Elsevier B.V.; 2010 Mar;142:339–346. .

54. Pandey R, Khuller GK. Antitubercular inhaled therapy: opportunities, progress and challenges. J Antimicrob Chemother. Irwin; 2005;55:430–435. .

55. Patomchaiviwat V, Paeratakul O, Kulvanich P. Formation of inhalable rifampicin-poly(L-lactide) microparticles by supercritical anti-solvent process. Aaps Pharmscitech. Springer US; 2008;9:1119–1129. .

56. Mohanraj VJ, Chen Y. Nanoparticles - A review. Trop J Pharm Res. 2007;5:561–573.

57. Sridhar R, Ramakrishna S. Electrosprayed nanoparticles for drug delivery and pharmaceutical applications. Biomatter. 2013 Mar;3:1–12. .

58. Chakraborty S, Liao I-C, Adler A, Leong KW. Electrohydrodynamics: A facile technique to fabricate drug delivery systems. Adv Drug Deliv Rev. Elsevier B.V.; 2009;61:1043–1054. .

59. Patel RP, Patel MP, Suthar AM. Spray Drying Technology: an overview. Indian J Sci Technol. 2009. p. 44–47. .

60. Valo H, Peltonen L, Vehviläinen S, Karjalainen M, Kostiainen R, Laaksonen T, Hirvonen J. Electrospray Encapsulation of Hydrophilic and Hydrophobic Drugs in Poly(L-lactic acid) Nanoparticles. Small. WILEY-VCH Verlag; 2009 Aug;5:1791–1798. .

61. Wu Y, MacKay JA, McDaniel JR, Chilkoti A, Clark RL. Fabrication of elastin-like polypeptide nanoparticles for drug delivery by electrospraying. Biomacromolecules. American Chemical Society; 2009;10:19–24. .

62. Almería B, Deng W, Fahmy TM, Gomez A. Controlling the morphology of electrospray-generated PLGA microparticles for drug delivery. J Colloid Interface Sci. Elsevier Inc.; 2010;343:125–133. .

63. Zeng J, Xu X, Chen X, Liang Q, Bian X, Yang L, Jing X. Biodegradable electrospun fibers for drug delivery. J Control Release. Elsevier; 2003;92:227–231. .

64. De La Mora JF, Loscertales IG. The current emitted by highly conducting Taylor cones. J Fluid Mech. 1994. p. 155. .

65. Alfonso M. Gañán-Calvo. New microfluidic technologies to generate respirable aerosols for medical applications. J Aerosol Sci. 1999;30:S541–S542. .

66. Gañán-Calvo AM, Dávila J, Barrero A. Current and droplet size in the electrospraying of liquids. Scaling laws. J Aerosol Sci. 1997;28:249–275. .

67. Hartman RPA, Brunner DJ, Camelot DMA, Marijnissen JCM, Scarlett B. Jet break-up in electrohydrodynamic atomization in the cone-jet mode. J Aerosol Sci. 2000;31:65–95. .

68. Hogan CJ, Yun KM, Chen D-R, Lenggoro IW, Biswas P, Okuyama K. Controlled size polymer particle production via electrohydrodynamic atomization. Colloids Surfaces A Physicochem Eng Asp. Elsevier; 2007;311:67–76. .

69. Lassalle V, Ferreira ML. PLA nano- and microparticles for drug delivery: an overview of the methods of preparation. Macromol Biosci. Wiley Online Library; 2007;7:767–783. .

70. Valo H, Peltonen L, Vehviläinen S, Karjalainen M, Kostiainen R, Laaksonen T, Hirvonen J. Electrospray Encapsulation of Hydrophilic and Hydrophobic Drugs in Poly(L-lactic acid) Nanoparticles. Small. WILEY-VCH Verlag; 2009 Aug;5:1791–1798. .

71. Bain DF, Munday DL, Smith A. Modulation of rifampicin release from spray-dried microspheres using combinations of poly-(DL-lactide). J Microencapsul. 1999;16:369–385. .

72. Celikkaya E, Denkbaş EB, Pişkin E. Rifampicin carrying poly (D,L-lactide)/poly(ethylene glycol) microspheres: loading and release. Artif Organs. 1996;20:743–751. .

73. Coowanitwong I, Arya V, Kulvanich P, Hochhaus G. Slow release formulations of inhaled rifampin. AAPS J. 2008 Jun;10:342–348. .

74. Bamrungsap S, Zhao Z, Chen T, Wang L, Li C, Fu T, Tan W. Nanotechnology in therapeutics: a focus on nanoparticles as a drug delivery system. Nanomedicine. 2012. p. 1253–1271. .

75. Jonathan P. Owens, Mariam O. Fofana DWD. Cost-Effectiveness of Novel First-Line Therapeutic Regimens for Tuberculosis. Int J Tuberc Lung Dis. 2013;17:1–12. .

76. Jorgensen JH, Ferraro MJ. Antimicrobial susceptibility testing: a review of general principles and contemporary practices. Clin Infect Dis. 2009;49:1749–1755. .

77. Woods GL. Susceptibility testing for mycobacteria. Clin Infect Dis. 2000;31:1209–1215. .

78. NCCLS. Performance Standards for Antimicrobial Susceptibility Testing. Clin Lab Standars Inst - NCCLS. 2007;27:1–182. .

79. Terada H, Hirota K. Endocytosis of Particle Formulations by Macrophages and Its Application to Clinical Treatment. In: Ceresa B, editor. Mol Regul Endocytosis. 2012. .

80. Ohashi K, Kabasawa T, Ozeki T, Okada H. One-step preparation of rifampicin/poly(lactic-co-glycolic acid) nanoparticle-containing mannitol microspheres using a four-fluid nozzle spray drier for inhalation therapy of tuberculosis. J Control Release. Elsevier B.V.; 2009 Apr;135:19–24. .

81. Smith JP. Nanoparticle delivery of anti-tuberculosis chemotherapy as a potential mediator against drug-resistant tuberculosis. Yale J Biol Med. 2011;84:361–369. .

82. Mirzaee M, Owlia P, Mehrabi M. Comparison of the bactericidal activitiy of amikacin in free and liposomal formulation against Gram-negative and Gram-positive bacteria. Jundishapur J Nat Pharm Prod. DocS; 2009;4:1–7. .

83. Halwani M, Mugabe C, Azghani AO, Lafrenie RM, Kumar A, Omri A. Bactericidal efficacy of liposomal aminoglycosides against Burkholderia cenocepacia. J Antimicrob Chemother. 2007 Oct;60:760–769. .

84. Beaulac C, Sachetelli S, Lagace J. In-vitro bactericidal efficacy of sub-MIC concentrations of liposome-encapsulated antibiotic against gram-negative and gram-positive bacteria. J Antimicrob Chemother. 1998 Jan;41:35–41. .

85. Maretti E, Rossi T, Bondi M, Croce MA, Hanuskova M, Leo E, Sacchetti F, Iannuccelli V. Inhaled Solid Lipid Microparticles to target alveolar macrophages for tuberculosis. Int J Pharm. 2014;462:74–82. .

86. Bourissou D, Martin-Vaca B, Dumitrescu A, Graullier M, Lacombe F. Controlled Cationic Polymerization of Lactide. Macromolecules. 2005;38:9993–9998. .

87. Wilhelm O, Madler L, Pratsinis S. Electrospray evaporation and deposition. J Aerosol Sci. 2003;34:815–836. .

88. Mohamed F, Van Der Walle CF. Engineering Biodegradable Polyester Particles With Specific Drug Targeting and Drug Release Properties. J Pharm Sci. Wiley Online Library; 2008;97:71–87. .

89. Lee Y-H, Mei F, Bai M-Y, Zhao S, Chen D-R. Release profile characteristics of biodegradable-polymer-coated drug particles fabricated by dual-capillary electrospray. J Control Release. Elsevier B.V.; 2010;145:58–65. .

90. Van Nostrum CF, Veldhuis TFJ, Bos GW, Hennink WE. Hydrolytic degradation of oligo(lactic acid): a kinetic and mechanistic study. Polymer (Guildf). 2004 Sep;45:6779–6787. .

91. Agrawal S, Ashokraj Y, Bharatam P V, Pillai O, Panchagnula R. Solid-state characterization of rifampicin samples and its biopharmaceutic relevance. Eur J Pharm Sci Off J Eur Fed Pharm Sci. 2004;22:127–144. .

92. Bouapao L, Tsuji H. Stereocomplex Crystallization and Spherulite Growth of Low Molecular Weight Poly(L-lactide) and Poly(D-lactide) from the Melt. Macromol Chem Phys. WILEY-VCH Verlag; 2009 Jun;210:993–1002. .

93. Jeong J-C, Lee J, Cho K. Effects of crystalline microstructure on drug release behavior of poly(epsilon-caprolactone) microspheres. J Control Release. 2003;92:249–258. .

94. Freiberg S, Zhu XX. Polymer microspheres for controlled drug release. Int J Pharm. 2004;282:1–18. .

95. Tikhonov VE, Stepnova EA, Babak VG, Yamskov IA, Palma-Guerrero J, Jansson H-B, Lopez-Llorca L V, Salinas J, Gerasimenko D V, Avdienko ID, Varlamov VP. Bactericidal and antifungal activities of a low molecular weight chitosan and its N-/2(3)-(dodec-2-enyl)succinoyl/-derivatives. Carbohydr Polym. 2006 Apr;64:66–72. .

96. Kong M, Chen XG, Xing K, Park HJ. Antimicrobial properties of chitosan and mode of action: a state of the art review. Int J Food Microbiol. Elsevier B.V.; 2010 Nov;144:51–63. .

97. Melake NA, Mahmoud HA, Al-semary MT. Bactericidal activity of various antibiotics versus tetracycline-loaded chitosan microspheres against Pseudomonas aeruginosa biofilms. African J Microbiol Res. 2012 Jul;6:5387–5398. .

98. Liu H, Du Y, Wang X, Sun L. Chitosan kills bacteria through cell membrane damage. Int J Food Microbiol. 2004 Sep;95:147–155. .

99. Katsikogianni M, Missirlis YF. Concise review of mechanisms of bacterial adhesion to biomaterials and of techniques used in estimating bacteria-material interactions. Eur Cell Mater. 2004;8:37–57. .

100. Boks NP, Norde W, van der Mei HC, Busscher HJ. Forces involved in bacterial adhesion to hydrophilic and hydrophobic surfaces. Microbiology. 2008;154:3122–3133. .

101. Oliveira R 1952-, Azeredo J, Teixeira P, Fonseca AP. The role of hydrophobicity in bacterial adhesion. BioLine; 2001. p. 11–22. .

102. Drulis-Kawa Z, Gubernator J, Dorotkiewicz-Jach A, Doroszkiewicz W, Kozubek A. In vitro antimicrobial activity of liposomal meropenem against Pseudomonas aeruginosa strains. Int J Pharm. 2006 Jun;315:59–66. .

103. Sachetelli S, Khalil H, Chen T, Beaulac C, Sénéchal S, Lagacé J. Demonstration of a fusion mechanism between a fluid bactericidal liposomal formulation and bacterial cells. Biochim Biophys Acta. 2000 Feb;1463:254–266. .

104. Zhang L, Pornpattananangku D, Hu C-MJ, Huang C-M. Development of nanoparticles for antimicrobial drug delivery. Curr Med Chem. 2010 Jan;17:585–594. .

105. Nel AE, Mädler L, Velegol D, Xia T, Hoek EM V, Somasundaran P, Klaessig F, Castranova V, Thompson M. Understanding biophysicochemical interactions at the nano-bio interface. Nat Mater. 2009;8:543–557. .

106. Fröhlich E. The role of surface charge in cellular uptake and cytotoxicity of medical nanoparticles. Int J Nanomedicine. 2012;7:5577–5591. .

107. Repnik U, Turk B. Lysosomal-mitochondrial cross-talk during cell death. Mitochondrion. Mitochondria Research Society; 2010;10:662–669. .

108. Gur G, Yarden Y. Enlightened receptor dynamics. Nat Biotechnol. 2004;22:169–170. .

109. Jiang W, Kim BYS, Rutka JT, Chan WCW. Nanoparticle-mediated cellular response is size-dependent. Nat Nanotechnol. NATURE PUBLISHING GROUP; 2008;3:145–150. .

110. Atul Asati, Santimukul Santra, Charalambos Kaittanis and JMP. Localization, Surface-charge-dependent Cell Nanoparticles, Cerium Oxide. ACS Nano. 2011;4:5321–5331. .

111. Zaki NM, Nasti A, Tirelli N. Nanocarriers for cytoplasmic delivery: cellular uptake and intracellular fate of chitosan and hyaluronic acid-coated chitosan nanoparticles in a phagocytic cell model. Macromol Biosci. 2011;11:1747–1760. .

112. Onoshita T, Shimizu Y, Yamaya N, Miyazaki M, Yokoyama M, Fujiwara N, Nakajima T, Makino K, Terada H, Haga M. The behavior of PLGA microspheres containing rifampicin in alveolar macrophages. Colloids Surf B Biointerfaces. 2010 Mar;76:151–157. .

113. Agrawal a K, Gupta CM. Tuftsin-bearing liposomes in treatment of macrophage-based infections. Adv Drug Deliv Rev. 2000 Mar;41:135–146. .

114. Anes E, Peyron P, Staali L, Jordao L, Gutierrez MG, Kress H, Hagedorn M, Maridonneau-Parini I, Skinner M a, Wildeman AG, Kalamidas S a, Kuehnel M, Griffiths G. Dynamic life and death interactions between Mycobacterium smegmatis and J774 macrophages. Cell Microbiol. 2006 Jun;8:939–960. .

115. Sonawane A, Santos JC, Mishra BB, Jena P, Progida C, Sorensen OE, Gallo R, Appelberg R, Griffiths G. Cathelicidin is involved in the intracellular killing of mycobacteria in macrophages. Cell Microbiol. 2011;13:1601–1617. .

116. Lee J, Remold HG, Ieong MH, Kornfeld H. Macrophage apoptosis in response to high intracellular burden of Mycobacterium tuberculosis is mediated by a novel caspase-independent pathway. J Immunol. 2006;176:4267–4274. .

117. Yu X, Jiang G, Li H, Zhao Y, Zhang H, Zhao L, Ma Y, Coulter C, Huang H. Rifampicin stability in 7H9 broth and Lowenstein-Jensen medium. J Clin Microbiol. 2010; .

118. Mohanty S, Jena P, Mehta R, Pati R, Banerjee B, Patil S, Sonawane A. Cationic antimicrobial peptides and biogenic silver nanoparticles kill mycobacteria without eliciting DNA damage and cytotoxicity in mouse macrophages. Antimicrob Agents Chemother. 2013 May; .

119. Mohanty S, Mishra S, Jena P, Jacob B, Sarkar B, Sonawane A. An investigation on the antibacterial, cytotoxic, and antibiofilm efficacy of starch-stabilized silver nanoparticles. Nanomedicine Nanotechnology, Biol Med. 2012;8:916–924. .

120. Jena P, Mohanty S, Mallick R, Jacob B, Sonawane A. Toxicity and antibacterial assessment of chitosan-coated silver nanoparticles on human pathogens and macrophage cells. Int J Nanomedicine. 2012 Jan;7:1805–1818. .

121. Pandey R, Zahoor A, Sharma S, Khuller GK. Nanoparticle encapsulated antitubercular drugs as a potential oral drug delivery system against murine tuberculosis. Tuberc Edinburgh Scotl. Elsevier; 2003;83:373–378. .

122. Rosenthal IM, Tasneen R, Peloquin CA, Zhang M, Almeida D, Mdluli KE, Karakousis PC, Grosset JH, Nuermberger EL. Dose-ranging comparison of rifampin and rifapentine in two pathologically distinct murine models of tuberculosis. Antimicrob Agents Chemother. 2012;56:4331–4340. .

123. Verma RK, Germishuizen WA, Motheo MP, Agrawal AK, Singh AK, Mohan M, Gupta P, Gupta UD, Cholo M, Anderson R, Fourie PB, Misra A. Inhaled microparticles containing clofazimine are efficacious in treatment of experimental tuberculosis in mice. Antimicrob Agents Chemother. 2013;57:1050–1052. .

124. Muttil P, Kaur J, Kumar K, Yadav AB, Sharma R, Misra A. Inhalable microparticles containing large payload of anti-tuberculosis drugs. Eur J Pharm Sci. 2007;32:140–150. .

125. Verma RK, Agrawal AK, Singh AK, Mohan M, Gupta A, Gupta P, Gupta UD, Misra A. Inhalable microparticles of nitric oxide donors induce phagosome maturation and kill Mycobacterium tuberculosis. Tuberculosis. 2013;93:412–417. .

126. Parikh R, Dalwadi S, Aboti P, Patel L. Inhaled microparticles of antitubercular antibiotic for in vitro and in vivo alveolar macrophage targeting and activation of phagocytosis. J Antibiot (Tokyo). 2014;1–8. .

127. Misra A, Hickey AJ, Rossi C, Borchard G, Terada H, Makino K, Fourie PB, Colombo P. Inhaled drug therapy for treatment of tuberculosis. Tuberculosis (Edinb). 2010;1–11. .